Quaternary Science Reviews 282 (2022) 107445

Contents lists available at ScienceDirect

Quaternary Science Reviews

journal homepage: www.elsevier.com/locate/quascirev

Response of a low elevation carbonate lake in the Yucatan Peninsula (Mexico) to climatic and human forcings

Sarah E. Metcalfe [a, *], Jonathan A. Holmes [b], Matthew D. Jones [a], Roger Medina Gonzalez [c, 1], Nicholas J. Primmer [a], Haydar Martinez Dyrzo [a], Sarah J. Davies [d], Melanie J. Leng [e]

[a] School of Geography, University of Nottingham, Nottingham, NG7 2RD, UK
[b] Environmental Change Research Centre, Department of Geography, University College, London, WC1E 6BT, UK
[c] Campus de Ciencias Biólogicas y Agropecuarias, Universidad Autonoma de Yucatán, Mérida, Mexico
[d] Geography and Earth Sciences, Llandinam Building, Penglais Campus, Aberystwyth University, SY23 3DB, UK
[e] British Geological Survey, Keyworth, NG12 5GG, UK

ARTICLE INFO

Article history:
Received 16 November 2021
Received in revised form
24 February 2022
Accepted 26 February 2022

Handling Editor: P Rioual

Keywords:
Holocene
North America
Stable isotopes
Inorganic geochemistry
Maya
Drought
Palaeolimnology
Palaeoclimatology

ABSTRACT

The importance of climate change, specifically drought, across the Maya region in the northern Neotropics, remains a topic of lively debate. Part of this discussion hinges on the coherency of response to climatic variability across different archives and proxies. In this paper we present a 6600-year palaeolimnological record from Yaal Chac, a carbonate lake (known locally as a cenote) in the northern lowlands of the Yucatan Peninsula, < 2 km from the location of the previously published Aguada X'Caamal record. The Yaal Chac sequence has been analysed for loss-on-ignition (LOI), stable isotopes ($\delta^{18}O$, $\delta^{13}C$) and elemental analysis using μXRF, complemented by some mineralogical, charcoal and pigment data. Mid Holocene sediments, predating evidence of human impact, are carbonate dominated and finely laminated. $\delta^{18}O$ values are positive (>2‰), but show no covariation with $\delta^{13}C$. A major transition occurs at ca. 4360 cal yr BP, with a change to generally more organic sediments and increased variability in all proxies. Although direct evidence for anthropogenic activity in the Yaal Chac catchment is limited, it seems feasible that human impact was affecting the system. Comparison with other records from the Northern Maya lowlands and the wider region shows little coherence in the mid Holocene, when Yaal Chac seems to have been quite stable, but possibly responsive to increased climatic seasonality, driving the production of seasonal laminae. In the late Holocene, when the climate was generally more variable, there is more coherence between Yaal Chac and other regional records, including the so called Pan Caribbean Dry Period (3500–2500 cal yr BP) and the droughts of the late Pre-Classic period (1800–1600 cal yr BP). The Yaal Chac record shows no evidence of drought at the time of either the Maya 'hiatus' or the Maya 'collapse' of the Terminal Classic, but does record drying from the 14th to 19th centuries CE, in keeping with other proxy and historical records. This new record from Yaal Chac highlights the spatial variability of responses to climate forcings and the importance of recognising individual system sensitivity.

© 2022 The Authors. Published by Elsevier Ltd. This is an open access article under the CC BY license (http://creativecommons.org/licenses/by/4.0/).

1. Introduction

Lake sediment sequences provide valuable, if sometimes complex, records of climatic change and human activities. Climatic and anthropogenic forcing can alter the chemistry, physical structures and biology of a lake both directly and indirectly (Fritz, 2008; Leavitt et al., 2009; Mills et al., 2017) and the interaction of these forcings, together with catchment specific factors, can lead to complex and spatially variable responses in sediment records

* Corresponding author.
E-mail addresses: sarah.metcalfe@nottingham.ac.uk (S.E. Metcalfe), j.holmes@ucl.ac.uk (J.A. Holmes), matthew.jones@nottingham.ac.uk (M.D. Jones), rmedina@correo.uady.mx (R.M. Gonzalez), sjd@aber.ac.uk (S.J. Davies), mjl@bgs.ac.uk (M.J. Leng).
[1] retired.

https://doi.org/10.1016/j.quascirev.2022.107445
0277-3791/© 2022 The Authors. Published by Elsevier Ltd. This is an open access article under the CC BY license (http://creativecommons.org/licenses/by/4.0/).

within and between lakes. For palaeoclimatic reconstruction, spatially uniform, or at least spatially structured, responses across a number of lake systems are most desirable, but these may be overridden by lake and catchment specific factors (Webster et al., 2000; Roberts et al., 2016), thus making it difficult to use lake-sediment records for regional climate reconstruction. There are then further challenges when attempting to make linkages between past climates and possibly related cultural changes. Our ability to reconstruct past climate and/or anthropogenic activity from individual lake sites rests in part on a detailed understanding of the ways in which different types of lakes respond to different factors, or differently to the same factors.

The Yucatan Peninsula (YP), within present day south east Mexico, Belize and northern Guatemala (~17–21°N, 87–92°W) (Fig. 1), supports numerous lakes (Perez et al., 2011) including cenotes and aquadas (see 1.1 for definitions), with proxy records that have been interpreted in terms of changing climate (Hodell et al., 1995; Leyden et al., 1996), human impact, or both (Leyden et al., 1998; Leyden, 2002; Anselmetti et al., 2007; Wahl et al., 2014; Torrescano-Valle and Islebe, 2015) during the mid to late Holocene. The YP is famous for being one of the core regions of pre-Hispanic Maya culture, which came to dominate a large part of Mesoamerica during the Classic period (ca. 250–1050 CE). The relationship between the Maya, the natural environment and climate, especially drought, has long been debated, specifically in relation to periods of major cultural change (Dunning et al., 1998; Aimers and Iannone, 2014).

Here we present a new record from Yaal Chac (20°35′N, 89°42′W, 7 m a.s.l.), a carbonate lake, locally referred to as a cenote, in the northern lowlands of the YP, Mexico, spanning the last 6600 years. Our study site lies <2 km south of the Aguada X'Caamal (Hodell et al., 2005a) (Fig. 1b) offering the opportunity to compare records from two adjacent sites, which can be assumed to have been subject to the same climatic forcings. We consider the Yaal Chac record based on a range of proxies, before making comparisons across the wider YP region and considering the implications of our findings for future lake sediment studies and their application.

1.1. Background to the study region

The Yucatan Peninsula is mainly a semi-emergent carbonate platform, comprising limestones, dolomites and evaporites. The northern and central parts of the YP reach less than 150 m a.s.l. (much of it less than 40 m a.s.l.), while the southern part can reach 400 m a.s.l. (Fig. 1a). Given its latitude and generally low elevation, the climate of much of the peninsula is warm, sub-humid (Köppen AW). It receives most of its precipitation in the summer (May to October), associated with the strengthening of the NE Trade Winds and associated easterly flows as the Inter Tropical Convergence Zone (ITCZ) moves northwards, and convection over the marine

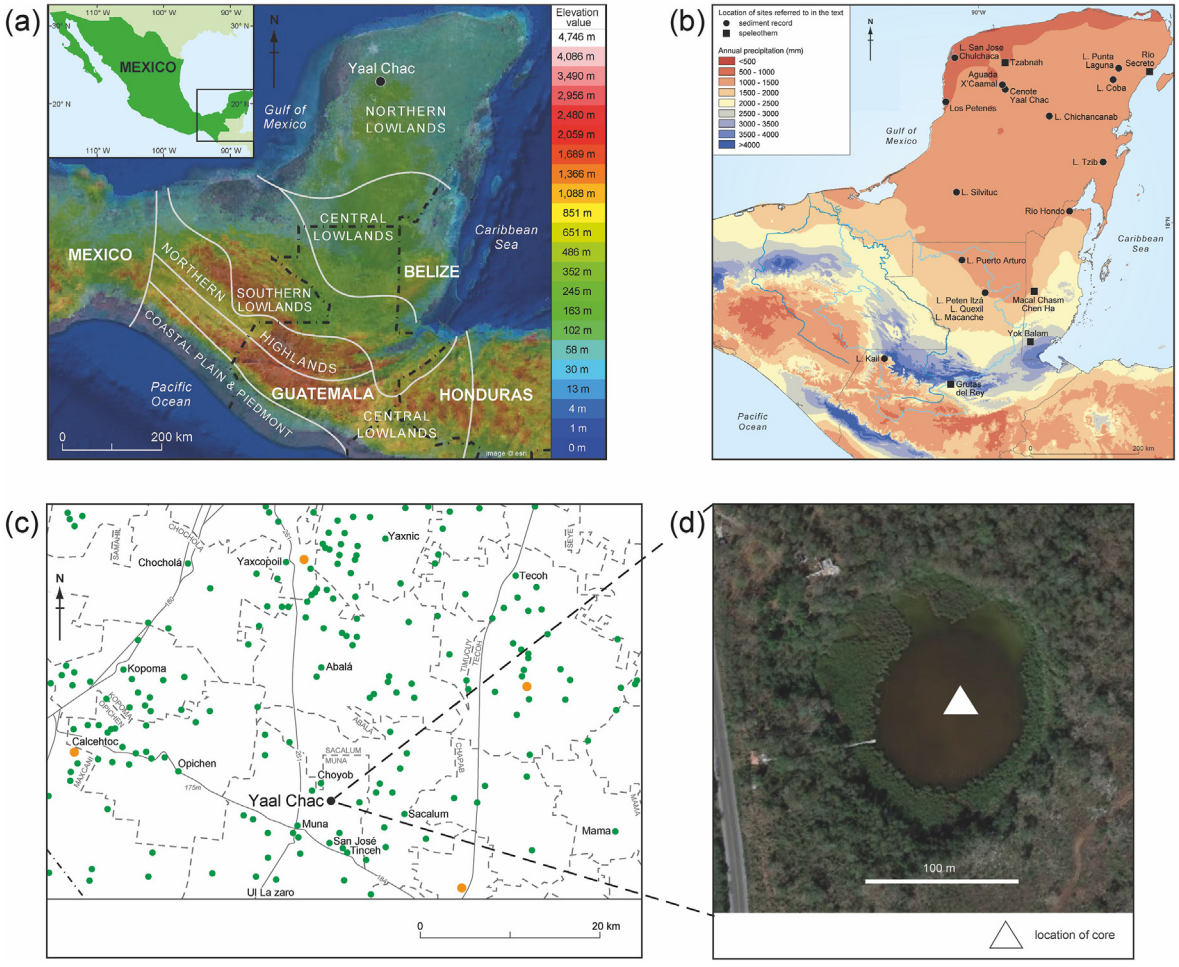

Fig. 1. a) Location of the Yucatan Peninsula, major physiographic features and Maya regions, b) Precipitation across the Yucatan Peninsula and the locations of lake/swamp and speleothem records referred to in the text, c) Distribution of Maya settlements in the area of Yaal Chac, green = minor, yellow = intermediate, from Witschey and Brown (2010), d) Image of Yaal Chac taken from Google Earth. (For interpretation of the references to colour in this figure legend, the reader is referred to the Web version of this article.)

western hemisphere warm pool. Tropical cyclones originating over the Caribbean/Gulf of Mexico can also bring significant amounts of precipitation in the late summer and autumn. Winters are generally dry, but cold fronts known as 'nortes', can bring some precipitation (De la Barreda et al., 2020). There is a strong gradient in total precipitation across the YP, from <300 mm in the NW, to >1800 mm in the south (Fig. 1b). Precipitation amounts are highly variable from year to year, as well as spatially, and the region is prone to droughts as evidenced in both the historical (Mendoza et al., 2006) and instrumental records (CONAGUA, 2014; De la Barreda et al., 2020).

The hydrology of the peninsula is profoundly affected by its geology including the effect of the Cretaceous/Palaeogene (K/Pg) boundary age Chicxulub impact, with its centre just off the modern north coast (Bauer-Gottwein et al., 2011). There are no permanent streams in the northern part of the YP and only limited numbers further south (e.g. in Belize) (Perry et al., 2003). There is however a very extensive, but thin, freshwater aquifer, overlying saline water, which is a vital water source for the region. The depth to the water table ranges from less than 10 m in the north, to more than 125 m in the south (Bauer-Gottwein et al., 2011). In spite of the general lack of surface water there are a large number of solution lakes ('cenotes') in the northern part of the YP and structurally controlled (often fault aligned) lakes further south. The latter include Lake Chichancanab (or Chichankanab) (Mexico) and Peten Itzá (Guatemala). There is a particular concentration of cenotes around the southern rim of the Chicxulub impact crater known as the 'ring of cenotes'. Cenotes show variable degrees of connectivity to the underlying water table, and may be lotic (well connected) or lentic (with more limited interchange). Lentic cenotes are sometimes called aguadas (although some aguadas may be artificial features). Lotic and lentic cenotes have very distinctive characteristics in term of sediment accumulation, chemistry and stratification (Schmitter-Soto et al., 2002).

The possible role of sea level change in driving hydrological change in the Maya lowlands must also be considered. Khan et al. (2017) report a lack of data for Mexico prior to 6900 cal yr BP, but the data from Belize, which extend back further, indicate that sea level was at about −17.3 m at 9400 cal yr BP rising rapidly through the early Holocene until about 6100 cal yr BP. Sea level then rose more slowly through to the present day. The modern aquifer (see above) is supported by the present sea level and it is known that only the deepest lakes in the YP (such as Peten Itzá, Mueller et al., 2010) were maintained through the last glacial maximum and into the early Holocene. As sea level and the local water table rose, so lakes refilled from around 9000 cal yr BP (e.g. Hodell et al., 1995; Leyden et al., 1998; Carillo Bastos et al., 2010).

1.2. The Maya, drought and palaeolimnology

Although it is agreed that the Classic Maya period population was large, different views are expressed about the extent to which they caused profound alterations to the natural environment (major vegetation change, enhanced soil erosion, changes in water quality) and how far they actively attempted to manage these issues (e.g. Rice and Rice, 1984; Dunning and Beach, 1994; Pohl et al., 1996; Ford, 2008). Even more contentious has been the extent to which the Maya were vulnerable to climate change, specifically drought. Major cultural dislocations in the lowland Maya region have been identified as occurring around 536–590 CE and again between ca. 750–1050 CE; these have been called the Maya 'hiatus' and the Maya 'collapse' respectively (Aimers and Iannone, 2014). Initial, rather blunt, differences between the perspectives of the palaeoclimatic and archaeological communities to the sensitivity of Maya to drought, have now become more nuanced (Aimers and Hodell, 2011). It is generally recognised that drought probably played some part in the 'hiatus' and the 'collapse', but that both the droughts and their impacts were spatially and temporally variable (e.g. Aimers, 2007; Dunning et al., 2012; Turner and Sabloff, 2012; Hoggarth et al., 2016; Douglas et al., 2016a).

The study of regional lake sediment records has played an important part in exploring the issues of climatic change, human impact and climate-human interactions across the Maya region (Fig. 1b). Pioneering work was carried out in the Peten region of northern Guatemala by Cowgill et al. (1966), in southern Mexico by Covich and Stuiver (1974) and then by Deevey and his collaborators (e.g. Deevey et al., 1979; Deevey et al., 1983). Brenner et al. (2002) provide a valuable synthesis of these earlier palaeolimnological studies. Originally, there was a significant bias towards pollen-based reconstructions, where late Holocene records are often clearly and strongly influenced by human activity. More recently stable isotope studies, particularly $\delta^{18}O$ in carbonate microfossils, have become increasingly common, as appropriate host material is abundant in the region's carbonate lakes. These records exploit the potential of this proxy to provide a record of water balance (P-E) change, and are less likely to be affected by humans than some other proxies. In the debate about the relationship between climate, specifically drought, and the Maya collapse, the record from Lake Chichancanab (Hodell et al., 1995) was seminal. This isotope approach has now been extended, particularly at Chichancanab, to include the use of δDwax (e.g. Douglas et al., 2015) and the application of a triple isotope approach ($\delta^{16}O$, $\delta^{17}O$, $\delta^{18}O$ and δD) to gypsum (Evans et al., 2018). It is notable that a number of these lake sediment stable isotope reconstructions have limited consideration of other proxies.

Although there is some coherence between the lake sediment isotope records from the YP, it is not always the case (Hodell et al., 2005a). The lack of a spatially uniform, or spatially structured isotope response (that would be a strong indication of a regional palaeoclimatic signal, see Introduction) and the possibility that isotope records may be affected by land use change (Rosenmeier et al., 2002, 2016), indicates that we still need to improve our understanding of the link between climate, hydrology and proxy systems across the Peninsula. This would lead to more informed consideration of the relationships between climatic variability and cultural change, of the type typified by the debates about the role of drought in societal change at the end of the Classic period.

2. Methods

Yaal Chac waters have been sampled on a regular, if not frequent (mainly once a year, occasionally monthly), basis since 2009 with a focus on chemistry and stable isotope composition (mainly oxygen and hydrogen), at the surface and in depth profiles through the water column. These data give some indication of the recent temporal and spatial variability in the lake system, including the degree to which it stratifies and how its trophic status varies. The changing stable isotope composition of the lake water provides important information on Yaal Chac's hydrology in terms of its degree of closure and probable isotopic sensitivity to climatic variability, specifically P/E (precipitation/evaporation).

Oxygen isotope ($\delta^{18}O$) measurements of waters were made at the stable isotope facility at the British Geological Survey (BGS) using the CO_2 equilibration method with an Isoprime 100 mass spectrometer plus Aquaprep device. Deuterium isotope (δD) measurements were made using an online Cr reduction method with a EuroPyrOH-3110 system coupled to a Micromass Isoprime mass spectrometer. Isotope measurements used internal standards calibrated against the international standards VSMOW2 and VSLAP2. Errors (external precision) are typically ± 0.05‰ for $\delta^{18}O$ and ±1.0‰ for δD. Some additional water analyses were carried out at the

University of Liverpool using a Picarro WS-CRDS system.

Local meteorological data are available from Abala (Conagua site 00031,001, 20° 39′ 03′′ N, 89° 40′ 49′′ W, 17 m a.s.l.) (https://smn.conagua.gob.mx), approximately 6.5 km NE of the lake. Monthly, if sometimes incomplete, records are available for Abala from 1968 to 2015, and are used here to compare with changes in the lake water chemistry.

A number of sediment cores (either overlapping, or parallel) have been collected from the basin, from a platform using a modified Livingstone corer to obtain long sediment sequences and from either a platform or a boat using a Glew corer to retrieve the surface sediments and sediment-water interface. All cores were taken in at least 10.5 m of water. Glew cores were sampled in the field at 1 cm intervals. Livingstone cores were either extruded and wrapped in the field (when using the conventional metal barrel), or retained in clear polycarbonate coring tubes. All sediment samples were sent by air back to the UK and then kept in cold storage (~4 °C). On return to the UK, intact cores were split vertically, photographed and described.

The Yaal Chac sediments present a very distinctive stratigraphy (see below) which allows for reliable visual matching between cores and core sequences. Here we present data from a long core sequence collected in 2011, with some additional material from a core taken in 2016, together producing a final composite core sequence of 297 cm.

A chronology for the full sediment sequence has been established using ^{14}C (9 samples) and ^{210}Pb methods. Radiocarbon dating was mainly carried out at the NERC Radiocarbon Laboratory at East Kilbride (UK). Although dating of terrestrial plant macrofossils is usually the preferred option in carbonate systems to avoid issues of hard water error, the lack of suitable plant material in the Yaal Chac cores precluded this. Dating of a surface sediment sample (SUERC-67887) yielded a modern date, with ^{14}C enrichment of 112.1 ± 0.51% so it appears that, at least today, dates based on bulk sediment are not affected by hardwater error. One radiocarbon date was obtained through Beta Analytic on a piece of wood. All ^{14}C dates are listed in Table 1.

Dried samples from the upper 30 cm of the core were analysed for ^{210}Pb, ^{226}Ra, ^{137}Cs and ^{241}Am by direct gamma assay in the Environmental Radiometric Facility at University College London (UK), using an ORTEC HPGe GWL series well-type coaxial low background intrinsic germanium detector. Following three weeks storage in sealed containers to allow radioactive equilibration, ^{210}Pb was determined via its gamma emissions at 46.5 keV, and ^{226}Ra by the 295 keV and 352 keV gamma rays emitted by its daughter isotope ^{214}Pb. ^{137}Cs and ^{241}Am were measured by their emissions at 662 keV and 59.5 keV (Appleby et al., 1986). Calibrated sources and sediment samples of known activity were used to determine the absolute efficiencies of the detector and corrections made for the effect of self-absorption of low energy gamma rays within the sample (Appleby, 2001). Results, based on the CRS model, are shown in Table S1. The final age model for the sediment sequence was created using Bacon (Blaauw and Christen, 2011) in R (R Core Team, 2020, version 2.4.1) with the default settings, generating ages in both cal yr BP and calendar years BCE/CE using Intcal13. Using Intcal20 makes no real difference over this time period given the resolution of our record (Reimer et al., 2020).

Table 1
Radiocarbon dates used to develop the Yaal Chac age model.

Lab number	Age ^{14}C year BP	δ^{13}C‰	Material dated	Core depth (cm)
SUERC-67887	Modern	−26.5	Bulk sediment	Surface sediment
SUERC-70339	831 ± 37	−29.1	Bulk sediment	40.5
SUERC-92921	1739 ± 37	−28.6	Bulk sediment	70
SUERC-70340	2296 ± 37	−29.8	Bulk sediment	97
SUERC-92926	2074 ± 37	−30.0	Bulk sediment	100
SUERC-92927	3072 ± 35	−31.4	Bulk sediment	140
SUERC-70341	3593 ± 37	−30.9	Bulk sediment	147
SUERC-70342	3673 ± 36	−29.7	Bulk sediment	216
Beta-29255	4420 ± 40	−28.1	Wood	237
SUERC-70343	5817 ± 37	−27.4	Bulk sediment	296

Intact cores were taken to Aberystwyth University for μXRF core scanning using their Cox Analytical ITRAX XRF core scanner (Croudace et al., 2006). Cores were scanned at 300 μm resolution, using a Molybdenum tube, with a count time of 15 s, at 30 kV voltage and a current of 30 mA for XRF measurements. XRF data are presented here normalised by incoherent scatter to minimise the impact of variable water and organic matter content on the raw elemental counts (Davies et al., 2015). For most subsequent analysis, these high resolution data were aggregated (using the pivot table function in Excel) into 1 cm increments to make them directly comparable with the other available data sets. The cores were then sampled at 1 cm resolution for loss-on-ignition (LOI; at 550 °C and 950 °C) to determine organic and carbonate content (after Dean, 1974) and stable isotope analysis.

Oxygen and carbon-isotope analyses of carbonate (δ^{18}O, δ^{13}C) were undertaken on 346 samples (including duplicates) at the Bloomsbury Environmental Isotope Facility (BEIF) in University College London (UCL). Although studies on other lake-sediment sequences from the YP have used carbonate fossils (ostracods or gastropods), these were inconsistently present at Yaal Chac, so we focused instead on endogenic carbonates. Bulk sediment samples were treated with 12% 'chlorox' at room temperature overnight to remove organic matter, rinsed and then sieved though a 125 μm sieve in order to remove shell material and thus isolate the fine fraction that is assumed to be endogenic. The fine fraction was dried and then analysed using a ThermoFinnigan Delta Plus XP mass spectrometer connected to a GasBench. Isotope values are reported in standard delta notation relative to the VPDB standard, with 1σ uncertainty of better than ±0.15‰ and ±0.10‰, for oxygen and carbon, respectively, across all of the analytical runs.

Each 1 cm level in the composite core sequence for which we had a full set of proxies (LOI, μXRF, δ^{18}O, δ^{13}C) was identified, yielding 216 samples. These core data were then zoned using the chclust (Coniss agglomeration method) stratigraphically constrained cluster analysis in the Rioja package in Rstudio (Juggins, 2019). In order to identify some patterns of behaviour in the data, the samples were also run through a Principle Components Analysis (PCA) using Canoco 5 (ter Braak and Šmilauer, 2012).

Some additional, low resolution, data for the 2011 core sequence, based on undergraduate student projects, are also used here. These data include: photosynthetic pigments using reversed HPLC and online photo diode array (PDA) spectrophotometry (45 samples) (following Chen et al., 2001) to indicate changes in algal and bacterial productivity and lake water transparency; charcoal (24 samples) (following Turner et al., 2010) to indicate burning (only microcharcoal >3 mm diameter used here) and XRD (24 samples) (using a Siemens D5000) to determine carbonate mineralogy, to underpin the stable isotope analysis and further improve our understanding of the system.

3. Results

3.1. Modern climatology

The meteorological record from Abala shows a pattern typical of most of Mexico, with a predominantly summer rainfall regime (especially June to October) (Fig. 2a). Mean annual precipitation over the period of record is 1084.4 mm, ranging from 677 mm to 1519.9 mm (for years with complete data). Mean annual

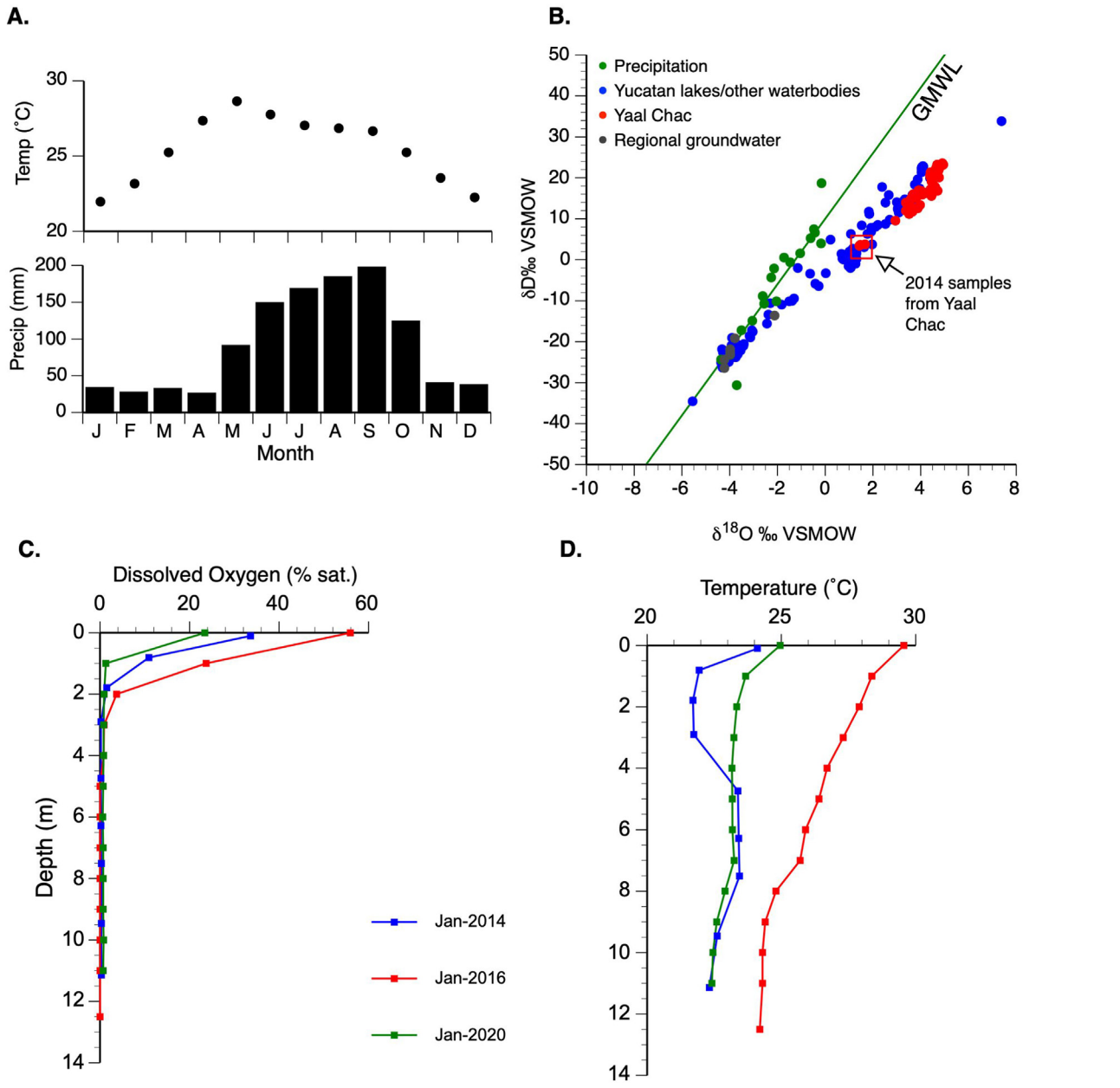

Fig. 2. a) Monthly average precipitation and temperature from Abala (data from Conagua, 1968–2016), b) Modern lake water isotope values from sites across the Yucatan Peninsula, c) Depth profiles of dissolved oxygen (% saturation) from Yaal Chac, d) Depth profiles of temperature (°C) from Yaal Chac.

temperature is 25.4 °C, with January the coldest month (average 21.9 °C) and May the warmest (28.6 °C). Mean annual evaporation is 1609.35 mm.

3.2. Modern limnology

Yaal Chac is a nearly circular sinkhole feature ca. 150 m in diameter, with no visible surface inflow or outflow (Fig. 1d). Although referred to as a cenote, its high EC (>5700 μS cm^{-1}), ionic composition (Na ≫ Mg > Ca, Cl ≫ SO_4=CO_3) and $\delta^{18}O$ values (+0.47 to +5.62‰) (Table 2) indicate that it is actually hydrologically closed and largely isolated from groundwater (a lentic cenote or aguada). Sampling of two local groundwater sites, with average $\delta^{18}O$ values of −3.5 and −4.1‰, highlights this difference between Yaal Chac and the groundwater. A comparison of surface water isotope values from Yaal Chac with those from other water bodies across the region (Fig. 2b) clearly indicates the position of Yaal Chac at the end of the local evaporation line. As Yaal Chac is currently a closed system, it seems very suitable for the application of stable isotope analysis to look at long term changes in water balance.

Both water chemistry and water isotope data highlight the period late 2013 to early 2014 as being unusual. $\delta^{18}O$ values were the lowest (less evaporated) recorded (<+2‰, from September 2013 to January 2014) (Fig. 2b), Mg and Na were present in more equal amounts and the predominance of $Cl^-$was reduced. These changes appear to be a response to unusually high precipitation from June to December 2013 (precipitation data for May 2013 were missing from the record, but the 11 month total for 2013 was 1327.5 mm compared with the long term average of 1084.4 mm). This indicates that the lake is responsive to changes in precipitation

Table 2
Basic parameters of Yaal Chac based on mid-lake surface samples (2009–2020).

Max depth (m)	Surface Temperature (°C)	pH	EC μS cm-1	Secchi transparency (m)	Dominant ions	$\delta^{18}O$ ‰ vs VSMOW	δD ‰ vs VSMOW
12–16	21.26–34.1	7.37–8.45	5700–8128	0.52–1.3	Na^+, Cl^-	+0.47 to +5.62[a]	+3.2 to +21.7@

@ values below +12‰ only recorded winter 2013-14.
[a] Values below +2‰ only recorded winter 2013-14.

amount in a way that may be captured in the lake sediment record. A similar sensitivity to extreme precipitation was noted in the adjacent Aguada X'Caamal in response to hurricane Isidore in September 2002 (Hodell et al., 2005a).

Water column profiles from the middle of the lake (usually 12–13 m water depth) indicate that Yaal Chac is generally meromictic recording a clear thermocline (at ca. 2 m in winter and ca. 4 m in summer) and oxycline (between 1 and 2 m) (Fig. 2c and d). There is occasional overturn in the winter months. Water temperatures are often quite stable below 6 m water depth and the water column is often anoxic below ca. 3 m water depth. Under most classifications of trophic status (including total P, chlorophyll *a* concentrations and Secchi depth) Yaal Chac is currently eutrophic.

3.3. Core record

The stratigraphy of cores from Yaal Chac is very distinctive, with a mix of finely laminated, carbonate dominated sediments (mainly 10 YR, 4/4 to 8/4 on the Munsell scale), very organic, dark units (mainly 10 YR 2/1 or 2.5Y 2.5/1) or banded sections with layers of more/less organic material and sometimes 'packets' of carbonate laminae. This distinctive visual stratigraphy, which has been replicated across a number of coring sites at Yaal Chac, allows a composite stratigraphy to be developed relatively easily. The visual correlation has been confirmed using the LOI data. The composite sequence for the 2011/2016 cores is illustrated in Fig. 3. The most notable feature of the Yaal Chac stratigraphy is that the basal part of the sequence (below 217 cm) is almost completely dominated by finely laminated, carbonate rich (60–82% $CaCO_3$) sediments. In the upper part of the sequence, although there are sections with clear carbonate bands and occasional laminae, the sediments are generally much more organic (30–83% TOC). Only towards the top of the core (mainly between 20 and 6.5 cm) are there multiple carbonate laminae more akin to those below 217 cm, although they still have highly organic sediments between them. Aragonite was important prior to ca. 6400 cal yr BP, but after this core carbonates are calcite dominated, mainly low Mg calcite, but with some periods of high Mg calcite.

The age-depth model (in cal yr BP) for the Yaal Chac sequence is shown in Fig. 4. All dates fall within the 95% confidence limits of the Bacon model. The age estimate for the base of the sequence is 6612 (6465–6752) cal yr BP with 95% confidence range. Plots of core data against age use the mean age estimate for each depth (red line in Fig. 4) in either calibrated years BP or CE/BCE.

The full core sequence is shown in Fig. 5, with 3 main zones and a number of sub-zones (most notably in Zone 2) identified using the output from chclust (see Methods). The principal division in the core record is that between Zone 1 and Zones 2 and 3, at ca. 4365 cal yr BP and the second division (between zones 2 and 3) at ca. 2160 cal yr BP. The initial outputs from the PCA indicated the overwhelming influence of LOI on the first axis, reflecting the basic split in the stratigraphy between the carbonate-rich lower part of the core and the more organic upper part (see above). To draw out some of the finer detail, the PCA was repeated excluding the LOI data (Fig. S1). The results of this second analysis are those referred to in this paper. Axis 1 on this second PCA (eigenvalue 0.48) was

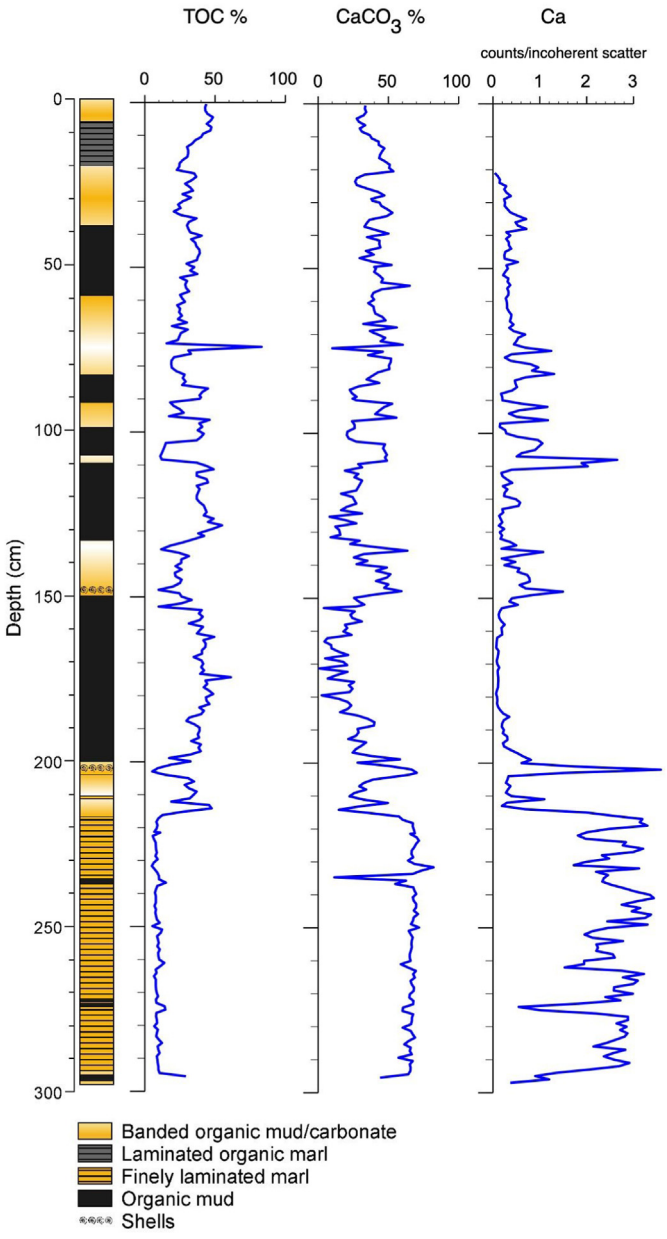

Fig. 3. Stratigraphy of the Yaal Chac core sequence (against depth), %TOC and %$CaCO_3$ based on LOI, Ca (counts/incoherent scatter).

driven by positive weightings on $\delta^{18}O$, $\delta^{13}C$, Ca, Sr and S and negative weighting for Br, while Axis 2 (eigenvalue 0.29) had positive weightings on Fe, Ti and Mn. Axis 3 (eigenvalue 0.11) separated out $\delta^{13}C$. Together these 3 axes explained 88.52% of the variation in the data. Downcore plots of the PCA axis scores (Fig. S1c) highlight the association with the main zones identified using chlust.

Zone 1 at the base of the sequence (6600–4360 cal yr BP) is the

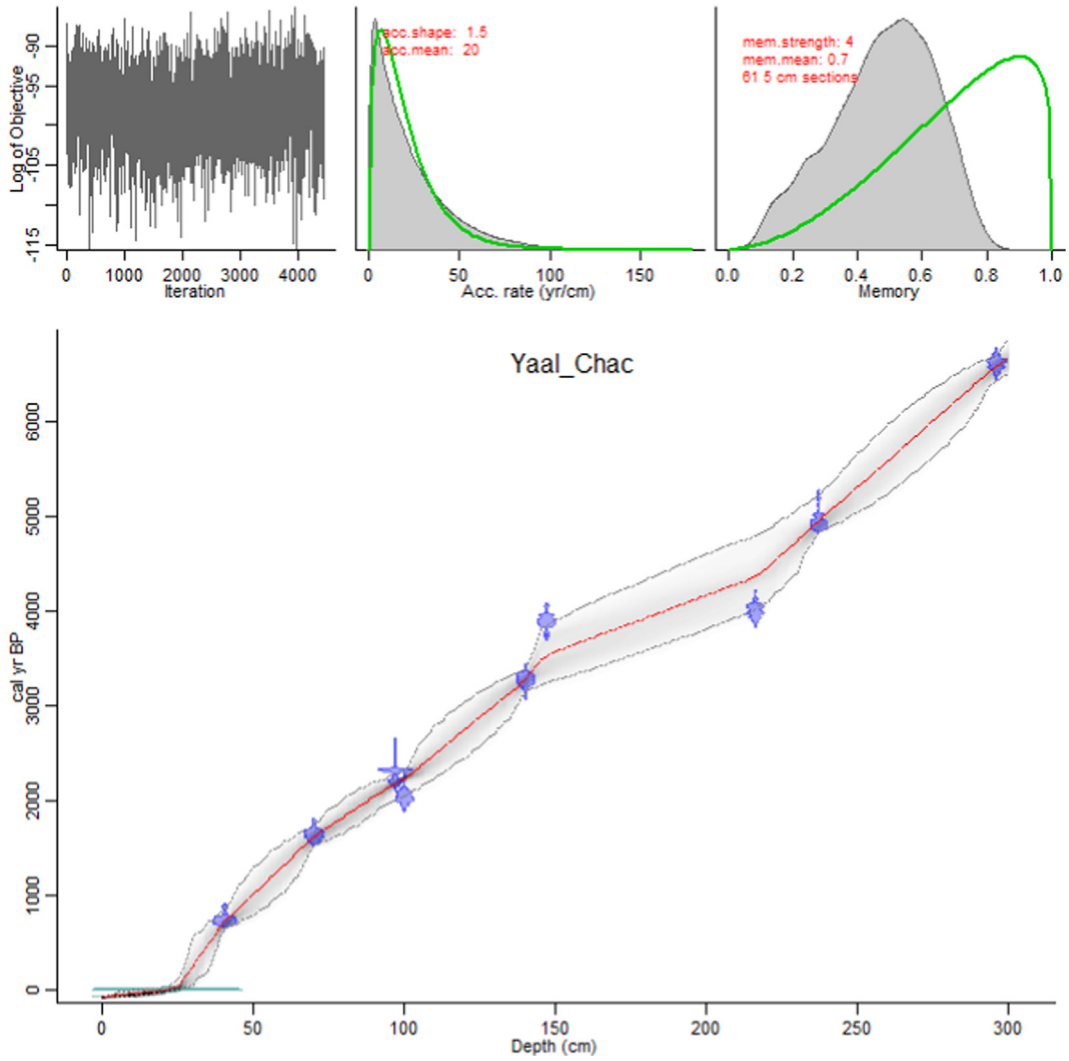

Fig. 4. Age depth model for the Yaal Chac sequence from Bacon.

part of the core that preserves clear laminations, some of which are thought to be annual (Primmer, 2019). It is marked by high % $CaCO_3$ (generally in the range 54.9–82.1%), high Ca and Sr and very positive values of $\delta^{18}O$ (+2.6 to +3.7‰), the highest of the entire record. $\delta^{13}C$ ranged between −1.1 and −4.2‰. S values are higher in this part of the core than in the rest of the sequence. Br values are low; Fe:Mn is high (but declining) while Fe is low. Proxy variability is generally low in this zone compared with other parts of the core sequence.

Zone 2 (4360–2160 cal yr BP) is marked by a very clear change from the basal, laminated marl into more organic-rich sediments, with some visible banding between more organic and more carbonate-rich sediments and 'packets' of carbonate laminae (e.g above the upper shell layer). The zone shows strong variability, recognised by the designation of 4 sub-zones, labelled 'a' to 'd', indicative of marked and quite rapid fluctuations in the system after the general stability of Zone 1.

Sub-Zone 2a (4360–4170 cal yr BP) shows marked changes within it, but is generally characterised by more organic sediments (generally >30% OM – organic matter), with the first clear peaks in Fe, Ti and Mn in the core record. $\delta^{18}O$ values drop sharply compared with zone 1 (−0.54 to +1.03‰), while $\delta^{13}C$ values are very variable. There is a switch to more carbonate-rich sediments at the top of this sub-zone, but this is not reflected in the $\delta^{18}O$.

Sub-Zone 2b (4170–3610 cal yr BP) is marked by high % of OM (mainly >40%), and low values of Ca, Sr, Fe, Ti, Mn and S. Fe:Mn is relatively high. Of the elements, only Br increases through this zone. $\delta^{18}O$ and $\delta^{13}C$ both decline to more negative values through 2b.

Sub-Zone 2c (3610–3110 cal yr BP) shows a return to more carbonate-rich sediments (peaking at 63.6% $CaCO_3$), with higher Ca, Sr and S than zone 2b. This zone is particularly distinctive for its high levels of Fe, Ti and Mn. $\delta^{18}O$ and $\delta^{13}C$ co-vary, showing a marked change to more positive values near the start of the zone, before becoming lower and more variable in a pattern than looks similar to the % $CaCO_3$.

Sub-Zone 2d (3110–2160 cal yr BP) is similar to zone 2b in its lower section, but switches to be more like Zone 2c around 2500 cal yr BP. In contrast to zone 2c, however, $\delta^{18}O$ remains low throughout, while $\delta^{13}C$ declines and then increases following the sharp increases in Mn, Ti and Fe. This lack of co-variability indicates different system behaviour from the earlier zone and is discussed further below.

Zone 3 (2160 cal yr BP - present). The break between Zones 1 + 2 and Zone 3 is the second in the hierarchy identified by cluster analysis (chclust). The general appearance of the sediments in this

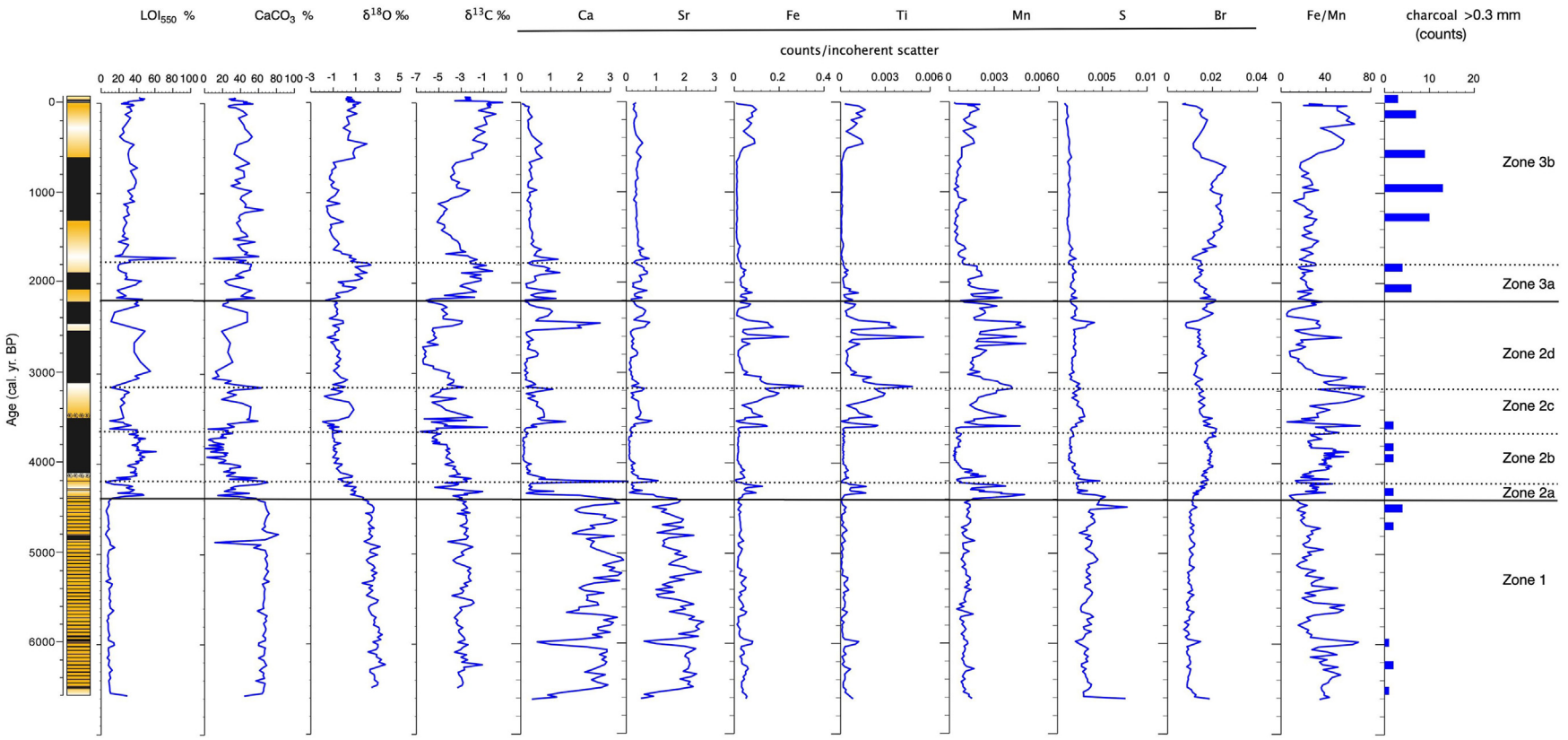

Fig. 5. Full Yaal Chac core sequence (against cal yr BP), with selected geochemical and isotope data zoned using chclust in the R package Rioja. Skeleton charcoal counts (>0.3 mm) also shown.

zone is quite similar to those in Zone 2, although the top of the sequence has a number of 'packets' of laminated sediments. Overall % of OM and $CaCO_3$ are intermediate compared with the rest of the core (OM mean 31.6%, $CaCO_3$ mean 40.7%) with less dramatic fluctuations. Chclust divides Zone 3 into two subsections.

Sub-Zone 3a (2160–1720 cal yr BP) is distinguished by high values of both $\delta^{18}O$ and $\delta^{13}C$ (maximum values + 2.35‰ and −0.21‰ respectively), reverting to a pattern of overall co-variation (unlike Zone 2d).

Although Sub-Zone 3b (1720 cal yr BP to present) displays evident variability in some proxies, there is no clear basis from the Chclust output for the formal designation of additional subzones, although changes are identified at ca. 1160 and 450 cal yr BP. The onset of this zone is marked by a sharp drop in values of $\delta^{18}O$ and $\delta^{13}C$ compared with Zone 3a and a sharp increase in Br. Levels of Fe and Ti are extremely low. After about 1160 cal yr BP, $\delta^{13}C$ begins to increase, a trend which generally continues until about 45 years ago. $\delta^{18}O$ also increases, but does not co-vary in a consistent way with $\delta^{13}C$, although both show a trend to more positive values from about 700 cal yr BP until ca. 450 cal yr BP. The most positive values occur at ca. 460 cal yr BP, +1.99‰ $\delta^{18}O$ and −0.70‰ for $\delta^{13}C$. The period after about 450 cal yr BP is marked by clear peaks in Fe, Ti and Mn and $\delta^{13}C$ values reach the highest values of the entire record (+0.68‰). After ca. 1970 CE $\delta^{13}C$ shows a sharp shift to lower values (−2‰ or lower) corresponding to an increase in % OM.

4. Discussion

4.1. Yaal Chac and the Northern Maya Lowlands

Based on a longer core from Yaal Chac we know that lacustrine deposition had started here by ca. 8800 cal yr BP (Primmer, 2019) so by the start of our record, the lake was well established.

4.1.1. Middle Holocene

The earliest part of the Yaal Chac record (Zone 1, 6600–4360 cal yr BP) is very different from the rest in terms of both its visual appearance (Fig. 3) and the behaviour of almost all the proxies employed. There is no evidence for catchment disturbance in this part of the Yaal Chac sequence, with low values of Ti and Fe. A small scale study of macrocharcoal showed the lowest abundances in this part of the Yaal Chac sequence (Fig. 5), also suggesting minimal anthropogenic activity in the catchment. Unfortunately we have no reliable pollen record from this site, but Zone 1 predates any clear evidence for human impact (specifically the presence of pollen of *Zea mays*) in this region (Islebe et al., 2018), so anthropogenic activity can be excluded as a major driver of change during this period.

The values of Ca, Sr and $\delta^{18}O$ in Zone 1 are the highest of the full 6600 year record (Fig. 5, Figs. S2a and c), $\delta^{13}C$ is also high. These are reflected by high scores on PCA axis 1 (Fig. S1). The predominance of $CaCO_3$ is notable, so it is important to try to understand the processes driving this high level of carbonate precipitation compared to later periods in the record. Percentages of $CaCO_3$ in this zone exceed any found in a transect of modern surface sediments from Yaal Chac, where the maximum was 31.1%. The observation of clear euhedral crystals of needle-shaped aragonite and rhombic calcite in the Yaal Chac sediments (Primmer, 2019), supported by a lack of Ca:Ti co-variation through the core (Fig. S2b), means that the possibility that high levels of $CaCO_3$ reflect inwash from the catchment can be excluded. Over the period represented by Zone 1, sea level probably rose 1–2 m (Khan et al., 2017). It is possible that this, perhaps combined with higher rainfall (see below), led to an increase in Ca and HCO_3 ions in the water which could generate more calcite deposition driven seasonally by saturation conditions and/or high productivity (Valero-Garcés et al., 2014). This mechanism of increased ionic concentrations would, however, only be viable if Yaal Chac were more open to groundwater influence at this time, as has been suggested for the Aguada X'Caamal (Hodell et al., 2005a), but this is difficult to reconcile with the very high $\delta^{18}O$ values, which tend to suggest increased hydrological closure. The presence of aragonite laminae, alongside the positive $\delta^{18}O$ values, seems to indicate the most highly evaporated conditions of this sequence, at least on a seasonal basis. Such enhanced evaporative enrichment is also one potential driver of the endogenic carbonates that are more commonly deposited and preserved in this zone. Biplots of $\delta^{13}C$ against both Ca and $CaCO_3$ at cm scale (in this part of the core 1 cm represents about 30 years) indicate tight clustering of values in Zone 1 with very little variability compared to the rest of the core (e.g. Fig. S2e). This emphasises the stability of the system over decadal timescales in contrast to the clear seasonality evident in the laminations.

The preservation of laminations in this part of the core would tend to indicate the presence of anoxia at the sediment-water interface, restricting biological activity and hence bioturbation. As noted above, stratification and lack of oxygen at depth are common under modern conditions, but only in the deeper parts of the lake, >4m (section 3.2). Lake cores recovered from shallower water have not preserved similar laminations. The potential presence of anoxia may be supported by the high levels of S in this part of the core (Boyle, 2001). The occurrence of high Fe:Mn with low Fe and high S (Fig. 5, Fig. S2d) may indicate the precipitation of Fe sulphides under anoxic conditions (Engstrom and Wright, 1984). Ca and S are also highly correlated. A partial pigment record (Stephenson, unpublished) shows periodically high levels of UV absorbing compound and high UV index (Fig. S3) indicating that water transparency was high. This would be very different from present day conditions (see Table 2).

Laminated sediments have been recorded at other sites in the Northern Lowlands and further south in the Peten in the Central Lowlands (e.g. Deevey et al., 1983). In the Hodell et al. (1995) record from Chichancanab, laminated sediments (not described in detail) are noted to occur between ca. 7500 and 3200 cal yr BP, during a period of low $\delta^{18}O$ values (see below) and would therefore probably be related to deep water. In contrast, in a shallow water core from further south in the Chichancanab basin, Covich and Stuiver (1974) link organic rich laminae, with high Ca and $\delta^{18}O$ to a drier climate. In Coba, Leyden et al. (1998) report distinct laminae between about 6500 and 2500 cal yr BP and particularly between ca. 6000 and 3000 cal yr BP, although they are described as being >1 cm thick and more organic rich than those in Zone 1 of Yaal Chac and are assumed to be shallow water deposits. The authors note that carbonate laminae may form under conditions of high productivity, but that strong seasonality in the NH tropics in the early Holocene could also be involved. In the Peten, partly laminated sediments in Quexil and Macanche are attributed to lakes being deep and probably meromictic in the early-mid Holocene, prior to extensive Maya impact which caused more inwashing of allochthonous material from these higher relief catchments (Deevey et al., 1983). Although detailed descriptions of laminae are generally lacking from publications for the Yucatan region, shallow water deposits seem to have thicker layers and higher organic content, while fine, carbonate-rich laminae are usually attributed to deeper water conditions as has been reported elsewhere (Tylmann et al., 2013). This issue is discussed further below.

The application of stable isotope analysis to carbonates in lake sediment cores to reconstruct changes in water balance (P-E) and hence, potentially drought history, is most effective in lakes that are hydrologically closed and our modern sampling (see above and Fig. 2) indicates that this is the case for modern Yaal Chac. It was our

expectation, therefore, that Yaal Chac's isotope record would be indicative of regional changes in P-E and hence climate. When reconstructing downcore change, a key indicator of closed hydrological status is often the existence of co-variation between oxygen and carbon isotope values (Talbot, 1990; Li and Ku, 1997; Horton et al., 2016), but this is not true everywhere. Taking the core record as a whole, covariability does apply, although the relationship is rather weak ($r^2 = 0.28$). A biplot of the two isotopes and the results of the PCA of the core samples, however, indicate that the relationship between these two isotopes has varied over time (Fig. 6a).

The sediment $\delta^{18}O$ values in Zone 1 exceed the maximum theoretical value (+2.2‰) of calcite $\delta^{18}O$ precipitated in equilibrium with lake water based on our modern sampling in early summer ($\delta^{18}O_{lake}$ of 5.6‰ at 32 °C; Fig. 6b). Together with high carbonate deposition (aragonite and calcite), the high sediment $\delta^{18}O$ values are consistent with more intense evaporation (low P/E) either annually or seasonally (see below). Co-variability between $\delta^{18}O$ and $\delta^{13}C$ is, however, weaker here than in the other zones, with an $r^2 = 0.17$. This lack of strong co-variation between $\delta^{18}O$ and $\delta^{13}C$ in this zone is probably related to the general stability of the system at this time. Co-variation between $\delta^{18}O$ and $\delta^{13}C$ is generally driven by responses to a common driver, assumed to be lake residence time (Li and Ku, 1997), but in stable lake conditions, where residence time varies little if at all, then small changes to both $\delta^{18}O$ and $\delta^{13}C$ may be driven by other, isotope specific, drivers such as rainfall $\delta^{18}O$ or productivity (for $\delta^{13}C$), such that there is lack of co-variation in the isotope 'noise', compared to the broader residence time 'signal'. The preservation of finely laminated sediments seems to reflect persistent stratification/anoxia, possibly in relatively deep water (see above), although based on current stratification depths, lake levels could have been slightly lower than modern. This seems possible given the relatively positive $\delta^{18}O$ values through this zone.

Comparison with other northern lowland palaeoenvironmental records may provide some insight into general climatic conditions over this period and help to explain the Zone 1 conditions in Yaal Chac, although few of them extend back to 6600 cal yr BP (Fig. 1b). The record from the nearby Aguada X'Caamal (Hodell et al., 2005a), which is chemically similar to Yaal Chac and today is also considered to be largely hydrologically closed, does not capture much of the period of Zone 1. $\delta^{18}O$ values are relatively low in the ca. 200 years of the Aguada sequence that overlaps with Yaal Chac Zone 1 (Fig. 7), but whether this is due to a higher P:E or the fact that X'Caamal was a more open system at this time (or both), is not clear (Hodell et al., 2005a). Pollen and isotope evidence from cenote San Jose Chulchaca (Leyden et al., 1996) suggest relatively low P:E between 7050 and 6050 cal yr BP, followed by generally high P:E conditions from about 6050 cal yr BP through to ca. 3800 cal yr BP, reaching maximum wetness ca. 5800 cal yr BP, followed by a brief drying ca. 5400 cal yr BP. Further south, the long isotope record from Chichancanab (Hodell et al., 1995) shows that after initial lake filling, the period from ca. 7900 to 3200 cal yr BP has lower values of $\delta^{18}O$ compared to the late Holocene. A speleothem $\delta^{18}O$ record from the Maya Mountains in Belize (Pollock et al., 2016) indicates conditions with higher rainfall than present day between 6900 and 4700 cal yr BP. No speleothem records from the northern part of the Maya lowlands extend back this far.

At Coba, Leyden et al. (1998) report the expansion and diversification of the regional forest, with slightly more semi-evergreen taxa from about 6690 cal yr BP, followed by little change until forest clearance began c. 3650 cal yr BP. Pollen from Rio Hondo (Aragon Morreno et al., 2018) also suggest mesic, and relatively stable conditions between 5600 (the base of the Rio Hondo record) and 3650 cal yr BP, and the mid Holocene pollen from Lake Silvituc (Torrescano-Valle and Islebe, 2015) is also dominated by tropical forest taxa, although there are few samples from this site that overlap with Yaal Chac Zone 1. Higher precipitation and more fluvial activity are suggested from the Ca/Fe data from the Rio Hondo sequence.

The limited number of other records from the northern Maya

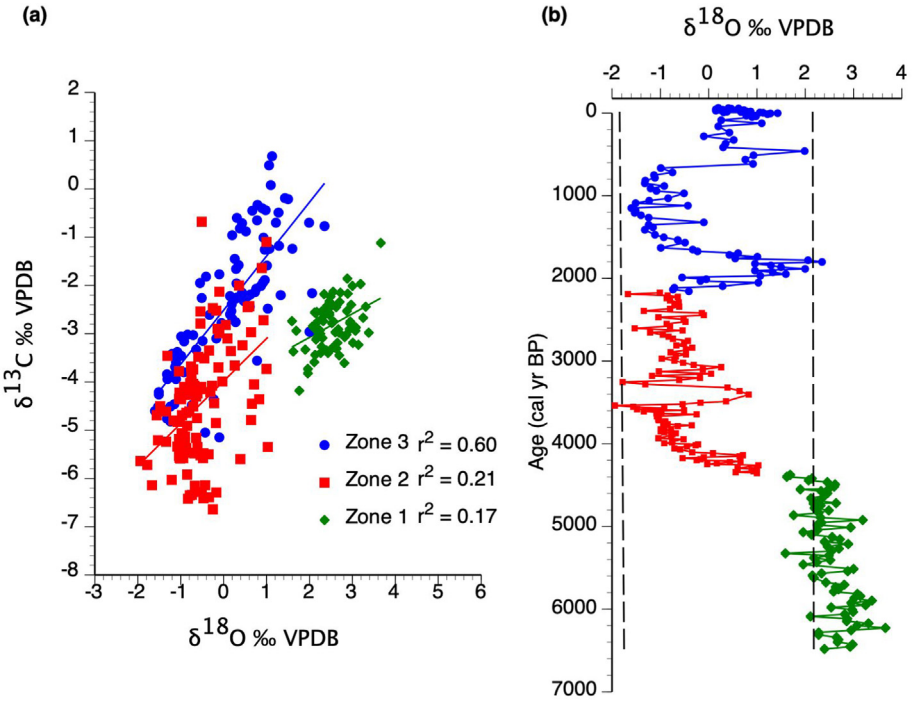

Fig. 6. a) Biplot of $\delta^{18}O$ vs $\delta^{13}C$ (by zone), b) Plot of downcore $\delta^{18}O$ with values based on maximum and minimum sediment values calculated from modern water samples and temperatures. Colours represent different zones. (For interpretation of the references to colour in this figure legend, the reader is referred to the Web version of this article.)

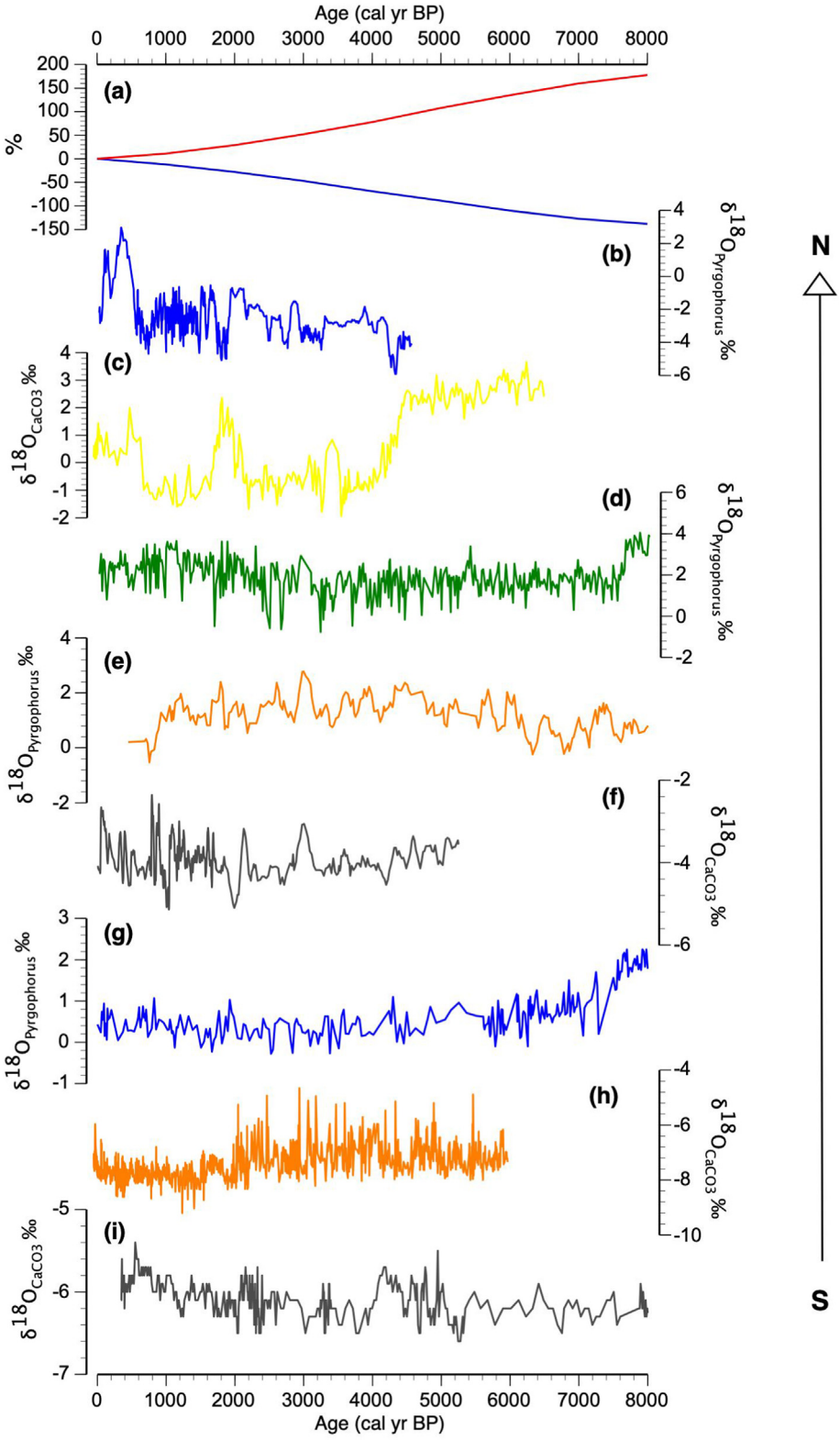

Fig. 7. Comparison of full Yaal Chac $\delta^{18}O$ record with other regional isotope records. a) Insolation at 20°N red (JJA), blue(DJF) (Berger and Loutre, 1991), b) Aguada X'Caamal (5 pt running average) (Hodell et al., 2005a), c) Yaal Chac (this study), d) L. Chichancanab (Hodell et al., 1995), e) L. Puerto Arturo (Wahl et al., 2014), f) Macal Chasm speleothem (Ackers et al., 2016), g) L. Peten Itzá (Curtis et al., 1998), h) Lake Kail (Stansell et al., 2020), i) Grutas del Rey Marcos speleothem (Winter et al., 2020). (For interpretation of the references to colour in this figure legend, the reader is referred to the Web version of this article.)

lowlands covering the Yaal Chac Zone 1 time period suggest a stable and mesic environment, with potentially higher rainfall than present day. If this were the case, then the very positive $\delta^{18}O$ values recorded in Yaal Chac Zone 1 may not be reflecting high annual E/P, but particularly enhanced evaporation in the dry season (spring), the probable time of carbonate precipitation. Combined with the other regional data, and other proxies from Yaal Chac itself that suggest water levels were not substantially lower than they are now, this points to an enhanced magnitude of seasonality in the mid Holocene, with an even clearer differentiation between dry and wet seasons than occurs today, under stronger insolation forcing (Fig. 7). This enhanced differentiation would enhance late dry season (spring) evaporation as suggested above. There is some evidence, based on the detailed examination of laminae in another core from Yaal Chac (Primmer, 2019), that annual dry season precipitation of carbonates was not occurring consistently in the early part of our Zone 1 (although $\delta^{18}O$ values were high), but then were annual through to the top of this zone. Yaal Chac may have been particularly sensitive to picking up the enhanced dry season conditions, rather than more average annual climate conditions, due to its small size and hydrological setting (c.f. Leng and Marshall, 2004; Jones and Imbers, 2010). Other possibilities are that the isotope signature has been influenced by inputs of more evaporated groundwater (Ito, 2001), or by catchment vegetation and its impact on catchment hydrology as suggested by Rosenmeier et al. (2016). Today, groundwater is much less evaporated than Yaal Chac itself (Fig. 2b), so this explanation would require significantly different conditions from present. If the catchment was covered in dense forest during this period (driven by wetter conditions and a lack of human impact), then it is possible that this actually had the effect of both reducing runoff and changing the isotopic signature of that runoff due to the preferential loss of ^{16}O through evapotranspiration. Pollen analysis from Yaal Chac would allow us to test this hypothesis.

4.1.2. Late Holocene

As described above and confirmed by the cluster analysis, the transition from Zone 1 to Zone 2 ca. 4360 cal yr BP is the most pronounced in the Yaal Chac record (Fig. 5). A switch in system behaviour seems to have occurred, something that is highlighted by biplots of a range of elements and oxygen and carbon isotopes (Fig. S2) where relationships in Zones 2 and 3 are very different from Zone 1. This is the point in the core where the stratigraphy changes from finely laminated, carbonate-rich sediments, to generally more organic sediments (Fig. 3). Zone 2 is itself very variable, reflected by the identification of 4 clear subzones and the potential for even finer subdivision. The most consistent feature of this zone is the presence of higher levels of Br than previously (Fig. 5). Absolute values of $\delta^{18}O$ and $\delta^{13}C$ are markedly lower than in Zone 1 and, for oxygen, fall within the expected range based on modern water temperature and isotopic composition (Fig. 6b), the covariance between the two isotopes is also different from Zone 1 (Fig. 6a). The correlation between $\delta^{18}O$ and $\delta^{13}C$ is slightly stronger than in Zone 1 ($r^2 = 0.21$), but this figure masks sharp differences between the sub-zones. It is weakest in 2a (then 2c) and strongest in 2b (then 2d); in 2b both $\delta^{18}O$ and $\delta^{13}C$ become more negative. Sub-Zones 2a and 2c are also marked by increases in elements that may indicate more inwashing of material from the catchment (Fe, Ti, Mn), as well as the highest values of the residual component of LOI (not shown) sometimes taken as an indicator of inputs of allochthonous material. This is reflected in high scores on PCA axis 2 (Fig. S1). The likelihood of increased disturbance and inputs of both detrital material and nutrients from the catchment is given some support by a gradual increase in macro-charcoal and clear increases in the abundance of the pigments chlorophyll *a*, β carotene, and echinenone (Fig. S3) indicative of overall in-lake productivity. This is consistent with the increase in Br which has been found to be associated with in-lake biological productivity (Gilfedder et al., 2011).

Over the period from 4360 to 2160 cal yr BP Yaal Chac and its catchment seem to have undergone rapid changes with periods of catchment stability and the accumulation of largely organic sediments, possibly under higher P:E conditions (Sub-Zone 2b) with renewed stratification (high Fe:Mn with low Fe), contrasting with instability and more carbonate-rich deposition. Within Sub-Zone 2c (3610–3110 cal yr BP) a transition from relatively stable catchment conditions, with the accumulation of carbonate sediments under a more evaporative regime, to one with more erosion could be envisaged. Sub-Zone 2d (3110–2160 cal yr BP) indicates continuing variability except in $\delta^{18}O$ which remains low. There is some similarity to the upper part of 2c, with renewed signs of disturbance after ca. 2700 cal yr BP.

Most of this zone coincides with the Preclassic period of Maya (and Mesoamerican) archaeology, but it extends back into the late Archaic. The earliest records of *Zea mays* in the Northern Maya Lowlands are found in this period, reported as early as 5600 cal yr BP at Rio Hondo (Aragon Morreno et al., 2018), ca. 4100 cal yr BP in Silvituc (Torrescano-Valle and Islebe, 2015), ca. 3500 cal yr BP in Lake Tzib (Carillo-Bastos et al., 2010) and ca. 2800 cal yr BP in Coba (Leyden et al., 1998). The establishment of large population centres gathered pace through the Middle Preclassic (ca. 950–400 BCE, 2800–2350 cal yr BP) and into the Late Preclassic (ca. 400 BCE – 300 CE, 2350–650 cal yr BP) when the first examples of large-scale public architecture emerged (Aimers and Iannone, 2014). At Coba, the pollen record is taken as indicating extensive *milpa* (traditional agriculture based on maize, beans and squash) from the Middle Preclassic onwards. It seems likely, therefore, that anthropogenic influence would have increased over this period.

Comparison with other records from the northern Maya lowlands (Fig. 1b) can give some indication of whether the Yaal Chac record is responding to climate over this period. For the period covered by Sub-Zones 2a and 2b, regional palaeoclimate records are rather mixed, with some indicating the persistence of conditions effectively wetter than present (e.g. Coba, Chichancancab), while at Rio Hondo, although more humid overall, drier conditions are reported at ca. 4300 and 4000 cal yr BP. A number of published records only start during this time period affecting the interpretation of relative wetness/dryness in the context of the full period of the Yaal Chac record. At Los Petenes, for example, which starts ca. 4095 cal yr BP, the period to 3930 cal yr BP is reported as relatively dry, with more disturbance vegetation (Guttierez-Ayala et al., 2012), before getting wetter until about 3400. This coastal site is, however, clearly affected by sea-level change. Elsewhere across the peninsula, away from the coast, it seems unlikely that the slow increase in sea level over the last 4000 years (Khan et al., 2017) would have had a major effect.

From around 3500 cal yr BP there is rather more consistency in the records with clear evidence of regional drying, which would be in keeping with our interpretation of Zone 2c. In the nearby Aguada X'Caamal, a gradual increase in $\delta^{18}O$ values from the base of the sequence (ca 4500 cal yr BP) shows a step increase at around 3100 cal yr BP (Fig. 7) (Hodell et al., 2005a). There seems to be a combination of both long term regional drying (e.g. Chichancanab, San Jose Chulchaca, Rio Hondo), increased variability and distinct drought periods (e.g. Silvituc). The record from Lake Punta Laguna (Curtis et al., 1996) only covers the last 3500 years and the period up to ca. 1700 cal yr BP is interpreted as relatively wet, but still with a number of very distinct drought periods. Conditions at the time of our Sub-Zone 2d are apparently rather variable, although the relative stability in $\delta^{18}O$ values in Yaal Chac contrasts with high

variability in $\delta^{18}O$ in the Aguada X'Caamal. Chichancanab has a period of gypsum precipitation (dry) between ca. 2750 and 2100 cal yr BP (Hodell et al., 2005b), while the Itzamna speleothem record from Rio Secreto (Medina-Elizade et al., 2016) shows conditions generally wetter than present from about 2950 cal yr BP (Middle Preclassic), followed by a distinct wet period in the Late Preclassic (ca. 2470–2116 cal yr BP), although interspersed with major drought episodes. One of these droughts between 531 and 516 BCE (2481–2446 cal yr BP) is estimated to have seen a reduction in precipitation of >50%. None of the lake records have the chronological resolution or precision of the speleothem record, so care must be taken in making inter-site comparisons, but it does seem that Zone 2 in Yaal Chac reflects both a more variable climate and possibly early human impact with the lake system fluctuating much more than during the deposition of Zone 1.

Zone 3 (2160 cal yr BP to present) in Yaal Chac appears less variable overall than Zone 2, except in relation to $\delta^{18}O$ and $\delta^{13}C$. In this zone, the correlation between $\delta^{18}O$ and $\delta^{13}C$ is the strongest in the core record ($r^2 = 0.60$) (Fig. 6a). The values of both these isotopes are high in Sub-Zone 3a (2160–1720 cal yr BP), but in contrast to Zone 1 these do not correspond with particularly high Ca, Sr, or % $CaCO_3$ (Fig. 5). In relation to these proxies, Sub-Zone 3a is similar to 2c, but with isotope values consistent with more evaporation. Sub-Zone 3a, however, differs markedly from 2c in its low Fe, Ti and Mn. Interestingly, there is no evidence in the Yaal Chac isotope record for major drought between ca. 1700 and 700 cal yr BP, which might relate to the Maya 'hiatus' or the 'Collapse', although there are some 'packets' of carbonate laminae through this period. The behaviour of $\delta^{13}C$ becomes increasingly distinctive through this zone as is reflected in PCA Axis 3 (Fig. S1). It seems likely, therefore, that more positive values of $\delta^{13}C$ may not only be responding to the effects of residence time and greater equilibration with atmospheric CO_2, but also to changes in aquatic productivity (Talbot, 1990; Leng and Marshall, 2004). Concentrations of most pigments, including echinenone (associated with cyanobacteria) increase in this part of the core (Fig. S3) and Br reaches its highest recorded levels. Although indicators of detrital inputs from the catchment are low, particularly through Sub-Zone 3b until ca. 450 cal yr BP, available charcoal data indicate a distinct increase in the abundance of large particles (especially those >0.3 mm in length) (Fig. 5) and there is some very preliminary pollen evidence (not shown here) indicating an increase in cultivated taxa (including *Zea mays*) over the last ca. 900 years.

Regionally, the period from ca. 1500 cal yr BP (~450 CE) saw major population growth and the establishment of large urban centres particularly in the Puuc area to the south and at T'ho (modern Merida) to the north. Although there were no major Maya sites in the immediate vicinity of Yaal Chac, there were a large number of small and medium size sites (e.g. at modern Yaxcopoil 17 km to the north) (Fig. 1c) (Witschey and Brown, 2010) and clearance of natural vegetation was probably widespread as population increased through the Classic period. It seems possible that the surrounding area was being cleared, but that erosion was limited, possibly because of the low relief of the catchment, thin soils and/or management practices (Sedov et al., 2007). Our age-depth model shows no sign of an increase in sedimentation rate over this period, in contrast to many sites in the central Maya lowlands where relief is higher and soils thicker (Beach et al., 2006). Although not formally recognised as a zone, there is a distinct change at ca. 450 cal yr BP, with evidence for renewed catchment erosion (Fe, Ti Mn). High Fe:Mn in this part of the core, in contrast to Zone 1, is probably controlled by erosion (Engstrom and Wright, 1984). The overall continued increase in $\delta^{13}C$ (independent of $\delta^{18}O$) may reflect further nutrient enrichment of the lake, increasing productivity and, in turn, leading to higher values of lakewater DIC and hence in the carbonate. This part of the core covers the period of Spanish colonisation, which progressed slowly, but by 1542 CE there was a permanent Spanish presence in the renamed city of Merida (Chamberlain, 1985). Although the population of the Yucatan may have dropped by around 70% by 1549 CE, largely as a result of the introduction of European diseases, it seems to have shown some recovery after 1580 CE and then grown significantly again from the late 18th century (Hoggarth et al., 2017). The disturbance apparent in most of the last 400 years of the Yaal Chac record may be related to changing landuse practices introduced by the Spanish, including cattle ranching.

To facilitate comparison with other records, the results for Zone 3 have been replotted against calendar years BCE/CE (Fig. 8). Sub-Zone 3a covers the period from ca. 200 BCE to 250 CE, most of the Late Preclassic. There are few other records from the Northern Maya lowlands that cover this period. At Punta Laguna, this is a period of transition to a drier climate, while in Chichancanab, there is a modest increase in gypsum precipitation ca. 100–200 CE and slightly elevated $\delta^{18}O$. The latter is consistent with our interpretation of drier conditions at this time, although there is no evidence of this in the Aguada X'Caamal record. As described above, Sub-Zone 3b in the Yaal Chac record shows no clear evidence for drier conditions at the time of either the Maya 'hiatus' or the Maya 'collapse'. The same is true in the nearby Aguada X'Caamal (Hodell et al., 2005a) (Fig. 1b). In contrast, both Punta Laguna and Chichancanab (Curtis et al., 1996; Hodell et al., 2005b) record a dry event at the time of the 'hiatus' and a more extreme series of droughts in the Terminal Classic (Fig. 9). The Chaac speleothem (near Merida) also records conditions drier than present around the time of the Maya 'hiatus' and very clearly at the time of the 'collapse' with a number of pronounced peaks 804–938 CE (Medina-Elizade et al., 2010). There is some indication of increased evaporation in the Yaal Chac record in the 14th and early 15th centuries. This is consistent with drought recorded in Punta Laguna and may be recorded in the Maya Books of Chilam Balam (Curtis et al., 1996). Drought has also been implicated in the abandonment of Mayapan in the mid 15th century (Aimers and Iannone, 2014). There is, however, no evidence for drought at this time in the Chaac speleothem. Possible enhanced evaporation in the 18th century would be consistent with historical droughts in this period (Hoggarth et al., 2017). The Aguada X'Caamal record indicates pronounced drying between the 15th and 19th centuries CE, which has been associated with the Little Ice Age (Hodell et al., 2005a).

Conditions at Yaal Chac during the late Holocene (represented by Zones 2 and 3) were distinct from those in the older Zone 1 and a change in system state seems to be indicated. Some of this could reflect increasing human impact (although evidence for this at Yaal Chac is limited until later in the record), but it is also possible that a change in climate state occurred. A transition in the northern Neotropics at around 4500 cal yr BP, has been widely reported (Mueller et al., 2009; Metcalfe et al., 2015; Aragon Morreno et al., 2018) with a general trend to drier and more variable conditions. The start of the zone is distinct and given the timing of Zone 2a (4354–4174 cal yr BP) its possible link to the global 'event' recognised at ca. 4200 cal yr BP cannot be excluded (Walker et al., 2012; Yan and Liu, 2019). As well as these climatic and anthropogenic drivers, there is also the possibility that local, hydrogeological conditions changed. At the end of Zone 1, the XRF data record an extreme spike in Cl (not shown) and a peak in S (Fig. 5). Considering the distance of Yaal Chac from the coast, this is unlikely to be due to general sea level rise, but it may reflect a change in groundwater routing, perhaps resulting in an incursion of Cl-rich water from the saline aquifer than underlies the peninsula (Escolero et al., 2005). Given the fractured nature of the bedrock in the Ring of Cenotes, this is feasible. Overall, the behaviour of Yaal Chac over the last

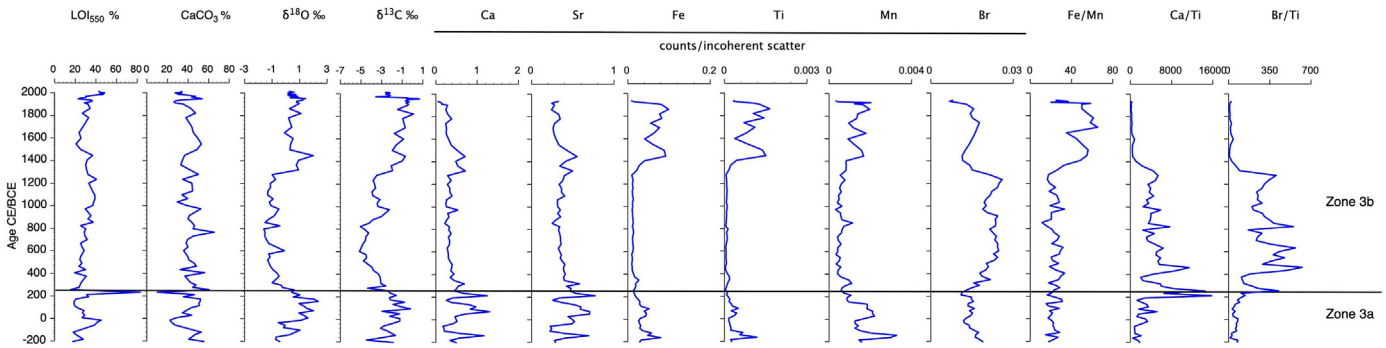

Fig. 8. Yaal Chac Zone 3 (plotted in years BCE/CE) selected geochemical and isotope data.

4200 years appears to be similar to the modern lake system, which monitoring has shown to be responsive to seasonal and interannual variations in precipitation. It seems reasonable, therefore, to accept that a combination of climatic and anthropogenic forcings are reflected in the down-core record over this period.

4.2. Yaal Chac in the wider region

As described in the Introduction, spatially uniform or spatially structured proxy responses between sites are most desirable for inferring palaeoclimate, but the individual characteristics of lakes and their catchments means that this is often not the case. Here we place the Yaal Chac record into its wider regional context and consider the implications of this for climate reconstructions and climate. Given the importance of stable isotope records to palaeoclimatology across the Yucatan Peninsula the Yaal Chac isotope record is compared with other lake and speleothem isotope records from the wider Maya region (Fig. 7). As noted in the comparison against other records from the Northern Maya lowlands (above), there is little obvious coherence between these and the Yaal Chac isotope record in Zone 1, but more coherence later in the record. Across the wider NH neotropics, the general interpretation in the early to mid-Holocene, is of conditions with higher precipitation and more effective moisture than present due to the northward displacement of the ITCZ and an enhanced summer monsoon in response to increased summer NH insolation (Fig. 7), although with some reduction in precipitation from about 6000 cal yr BP. There are some exceptions to this such as the record from Lake Kail (Guatemala) (Stansell et al., 2020) and Lake Antoine (Grenada) (Fritz et al., 2011, not on figure). The link between the Yaal Chac isotope record and range of potential forcing factors over this period (Fig. 10) is far from evident. This may reflect the fact that our isotope record from Zone 1 is seasonal rather than representing annual average conditions, being sensitive to enhanced seasonality in this period.

There are some features of the Yaal Chac Zone 1 record, however, which do seem to occur at other sites, particularly the deposition of laminated sediments (see above) and high % of $CaCO_3$. Percentages of $CaCO_3$ higher than those in the late Holocene are also recorded at other sites including Chichancanab (Hodell et al., 1995) and Puerto Arturo (Wahl et al., 2006), suggesting that neither Ca nor HCO_3 were limiting, perhaps in response to stronger groundwater flow and overall conditions wetter than present (see above) although neither may apply in the case of Yaal Chac. There is no doubt that the system as a whole was rather different from the later Holocene, with greater overall stability, perhaps making it less responsive to any broad-scale climatic variations. In this period it seems likely that catchment factors specific to Yaal Chac are masking any regionally coherent pattern.

Over the late Holocene, Yaal Chac seems to have experienced more variability, perhaps reflecting an increasingly variable climate system (Fig. 10). There does appear to be more coherence between Yaal Chac and regional records during this period than was the case earlier. The drying recorded from about 3500 to 2500 cal yr BP at other sites in the Northern Lowlands, is evident at sites across the wider region (Fig. 7), extending as far as Guatemala in the south (Stansell et al., 2020) to the Bahamas in the north (van Hengstum et al., 2018). Van Hengstum et al. refer to this as the Pan Caribbean Dry Period and suggest that it reflects a period of southward displacement of the ITCZ (see also Mueller et al., 2009). Low SSTs in the Eastern Equatorial Atlantic at this time (Fig. 10e) have been linked to a weakening of the African and Indian Monsoon systems and low lake levels across equatorial Africa (Weldeab et al., 2005). More broadly changes in SSTs, interhemispheric temperature differences and ITCZ position are indicated (Fig. 10), while ENSO strength was still relatively low. In this period, at least, climate forcing seems to drive a largely coherent regional response. Another time of coherence in a number of records is the period around 1800 -1600 cal yr BP, the Late Preclassic, when droughts were recorded across much of the Maya region (e.g. Wahl et al., 2014; Nooren et al., 2018). Medina Elizade et al. (2016) refer to a Late Preclassic Drought Event corresponding to the abandonment of several Mayan sites across the Peninsula. The period ca. 150–200 CE has been called the Maya abandonment and it has been argued (Dahlin, 1983) that drought played an important role in this, although this has been rejected by Aimers and Iannone (2014). Periods of drought in the Terminal Classic (Maya 'collapse') have been reported across the wider region (Kennett et al., 2012; Ackers et al., 2016), but is clearly not present in all records (Douglas et al., 2016a; Rosenmeier et al., 2016) or the drying was not anomalous (Wahl et al., 2014). In the historic period, the Macal chasm speleothem in Belize (Ackers et al., 2016) records major dry events in the 16th and late 18th/early 19th centuries CE consistent with records from the northern region, including the Aguada X'Caamal and Yaal Chac (Fig. 9).

5. Conclusions

Yaal Chac preserves one of the longer lake records from the Northern Maya lowlands, with evidence for climatic and anthropogenic drivers of change moderated by catchment specific factors. The differences between this record and that from the adjacent Aguada X'Caamal, and other sites across the northern Mayan lowlands, highlights the complex nature of lake sediment palaeoenvironmental records and the need for care when attempting to draw wider conclusions from individual, or even a limited number, of sites.

Regional climatic conditions in the mid Holocene, with high lake

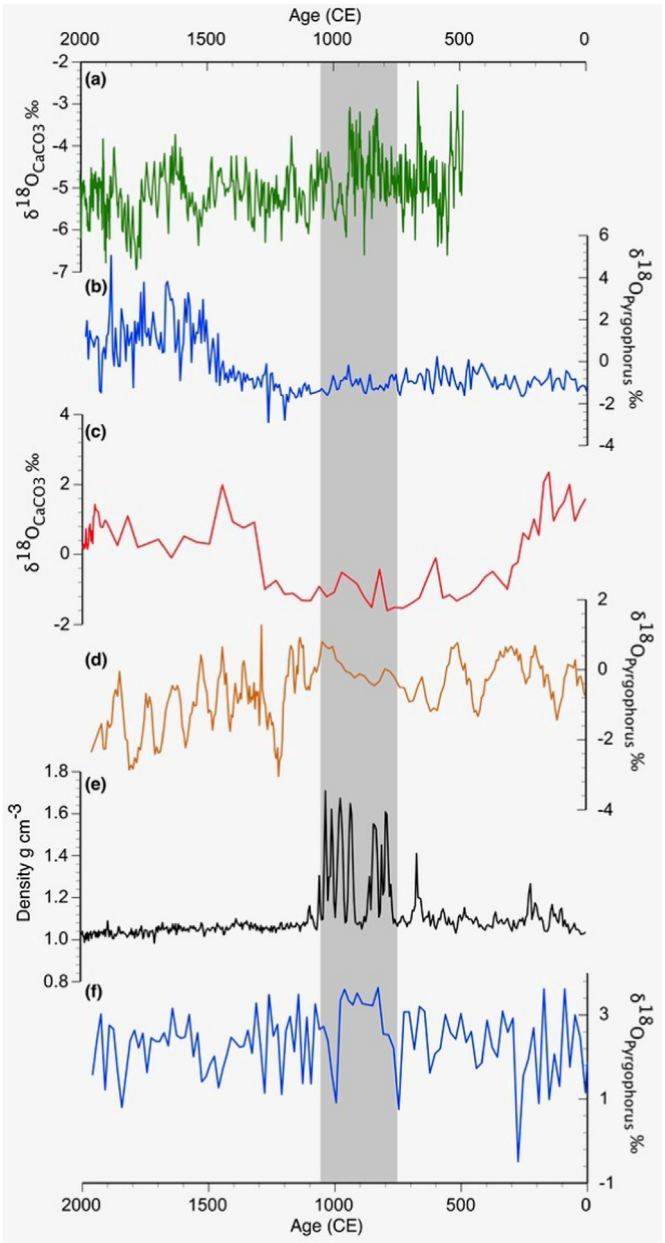

Fig. 9. Last 2k yr comparison of Yaal Chac with other records from the Northern Maya lowlands (plotted in years CE). a) Tzabnah speleothem $\delta^{18}O$ (Medina Elizade et al., 2010), b) Aguada X'Caamal $\delta^{18}O$ (Hodell et al., 2005a), c) Yaal Chac $\delta^{18}O$ (this study), d) Punta Laguna $\delta^{18}O$ (Curtis et al., 1996), e) L. Chichancanab density (Hodell et al., 2005b), f) L. Chichancanab $\delta^{18}O$ (Hodell et al., 1995). Period of the Maya 'Collapse', 750–1050 CE as described by Aimers and Iannone (2014), shaded in grey.

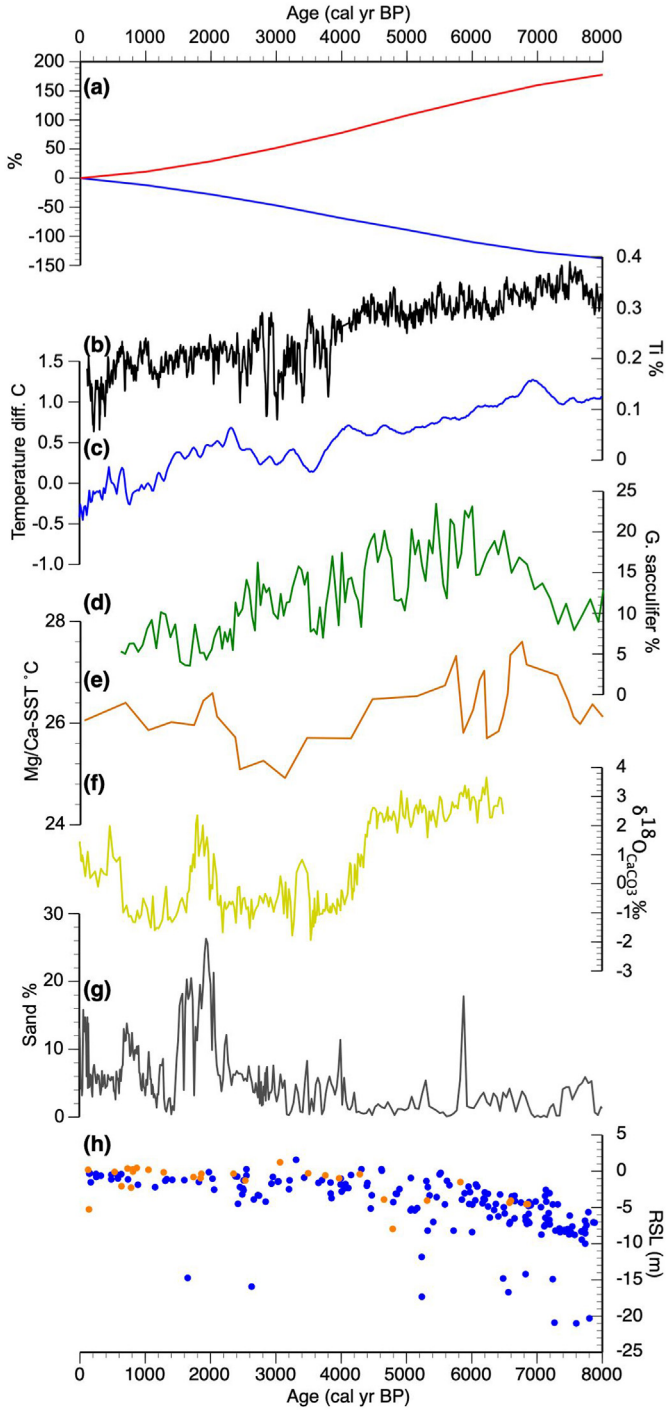

Fig. 10. Yaal Chac record compared with a range of records indicative of possible forcings: a) insolation at 20°N red (JJA), blue (DJF) (Berger and Loutre, 1991); b) Cariaco Basin Ti (Haug et al., 2001); c) Extra-tropical temperature difference (Marcott et al., 2013); d) % *G. sacculifer* from core RC12-10, Gulf of Mexico (Poore et al., 2003); e) SST reconstruction from Mg/Ca in core GeoB4905, Eastern Equatorial Pacific (Weldeab et al., 2005); f) $\delta^{18}O$ Yaal Chac (this study); g) % sand, El Junco (Conroy et al., 2008); h) relative sea level change for Belize (blue dots) and Mexico (orange dots) (Khan et al., 2017). Vertical dash line marks 4500 cal yr BP, grey shading indicates the Pan Caribbbean Dry Period (3500–2500 cal yr BP). (For interpretation of the references to colour in this figure legend, the reader is referred to the Web version of this article.)

isotope values, finely laminated sediments and high sediment carbonate content at Yaal Chac, remain somewhat uncertain. The Yaal Chac system appears to have been remarkably stable over this period, at least over decadal timescales, with the isotope signature appearing to be dry season specific, rather than capturing mean annual conditions. In looking to understand and fully interpret the Yaal Chac $\delta^{18}O$ system, this study has highlighted the need for better understanding of the processes of carbonate deposition in these tropical systems, be it as sediment or in different gastropod and ostracod species (sources of many key lake isotope records from this area (see Escobar et al., 2010)), and the impact of this on resulting core $\delta^{18}O$ records. Unlike many lakes in the tropics, we

have been able to accumulate quite a lot of data about the modern limnology of Yaal Chac, which has helped to put the earlier part of the record into context, although it has been of limited value in terms of serving as a direct analogue when the system state was clearly very different in the Mid Holocene. The application of other methods, such as pollen (for a local vegetation reconstruction) and diatom analyses (as a further potential proxy of lake depth and/or productivity), may help improve our interpretation of the early part of the record in particular and place it more confidently into the wider regional Middle Holocene context, itself somewhat understudied in this region.

There is a major transition at the start of the Late Holocene, probably driven by multiple factors. The timing of this transition is consistent with changes observed across the wider region and globally. Although it has been noted that the NH neotropics may not be as responsive to insolation forcing as other tropical regions, the increasing variability of the climate system after about 4500 cal yr BP is evident (Fig. 10), probably as other drivers of variability originating in the Pacific (ENSO) and the Atlantic (AMO) became more important (Bernal et al., 2011; Metcalfe et al., 2015; Winter et al., 2020). Increasing coherence of Yaal Chac with regional records over the late Holocene may suggest increased sensitivity of the system to this climatic forcing, in spite of, and maybe in part due to, evidence for increasing human impact.

The reconstruction of drought histories has played a central role in previous palaeoclimatic work on the YP and our understanding of the variability of these in space and time has increased (e.g. Douglas et al., 2015). The Yaal Chac record does not indicate drought conditions in the Terminal Classic, even though calculated precipitation amounts during the major droughts in this period have been estimated elsewhere to be between 36 and 54% below present (Medina-Elizade et al., 2010; Evans et al., 2018). The fact that drought rarely affects the whole peninsula should not be surprising given the regional variability visible in the available instrumental record (De la Barreda et al., 2020) and individual system sensitivity and location specific factors will always come in to play. The additional challenge of linking climate to people and socio-political transition is significant and needs to be done with care in the past, present and future (Aimers and Iannone, 2014; Douglas et al., 2016b; Kennett and Hodell, 2017). As well as being aware of how lake systems, indeed any climate archives, show different sensitivity to climatic and other forcings, so we need to be equally aware of how variable human/social vulnerability, adaptation and resilience can be (e.g. Chase and Chase, 2014; Metcalfe et al., 2020; Degroot et al., 2021). The complex relationships between meteorological and hydrological drought, access to scarce resources and social tensions all come in to play across the Maya region as elsewhere (e.g. Hoggarth et al., 2017; Jones et al., 2019; Arnold et al., 2021). Climate projections for the YP and the wider Central American region, indicate that drought is likely to become more prevalent (e.g. Colorado-Ruiz et al., 2018) affecting both natural and social systems. The study of the past can play a role in helping to understand what some of these impacts might be like, in terms of severity and spatial extent, but only if based on a thorough assessment of our records and their limitations.

Author contributions

Sarah Metcalfe, Jonathan Holmes and Matthew Jones developed the study and obtained funding to support the work; Roger Medina Gonzalez, Nicholas Primmer, Haydar Martinez Dyrzo, Sarah Davies and Melanie Leng all made important contributions of primary data. Sarah Metcalfe led on the authorship of the paper, but all authors contributed.

Data availability

Water isotope data collected under NERC NIGFSC; IP-1812-0618 are available in the NERC/BGS NGDC. Following publication all data will be made available via the NGDC and the NOAA Paleoclimate Data Center.

Declaration of competing interest

The authors declare that they have no known competing financial interests or personal relationships that could have appeared to influence the work reported in this paper.

Acknowledgements

NERC ^{14}C allocation 1724.0713, Dr. Handong Yang, UCL (^{210}Pb dating), NERC grants NE/K00610X/1 and NE/K004611/1 (Climate Variability over the circum-Caribbean region during the past 1200 years from oxygen isotope analyses of lake sediments), NERC NIGFSC IP-1812-0618 and IP-1394-1113, Santander Travel Fund award (University of Nottingham) (to SEM and MDJ), NERC Envision DTP studentship NE/L002604/1 (to SEM and MDJ for Nicholas Primmer), Dr. David Wahl USGS/UC Berkeley (Puerto Arturo data), Prof. Tapio Schneider CalTech for providing the NH-SH hemisphere temperature contrast data from Marcott et al. (2013), Prof. David Hodell University of Cambridge (Aguada X'Caamal data), Gemma Harwood (charcoal data), Mark Stevenson (pigment data), Prof. Walter Witschey Cook-Cole College of Arts and Sciences (shapefiles with Maya site data for the area around Yaal Chac). Other data sets were obtained from the IGBP/PAGES World Data Center for Palaeoclimatology. SEM would like to thank Dr. Mark Brenner University of Florida at Gainesville for many valuable exchanges about the lakes of the Yucatan and carbonates in particular. SEM and MDJ would also like to acknowledge the contributions of UoN Quaternary Environments students who got this work started.

Appendix A. Supplementary data

Supplementary data to this article can be found online at https://doi.org/10.1016/j.quascirev.2022.107445.

References

Ackers, P.D., Brook, G.A., Ralisback, L.B., Liang, F., Iannone, G., Webster, J.W., Reeder, P.P., Cheg, H., Edwards, R.L.(, 2016. An extended and higher-resolution record of climate and land use from stalagmite MC01 from Macal Chasm, Belize, revealing connections between major dry events, overall climate variability, and Maya socio-political changes. Palaeogeogr. Palaeoclimatol. Palaeoecol. 459, 268–288. https://doi.org/10.1016/j.palaeo.2016.07.007.

Aimers, J.J., 2007. What Maya collapse? Terminal classic variation in the Maya lowlands. J. Archaeol. Res. 15, 329–377. https://doi.org/10.1007/s10814-007-9015-x.

Aimers, J., Hodell, D., 2011. Drought and the Maya. Nature 479, 44–45.

Aimers, J., Iannone, G., 2014. The dynamics of Ancient Maya developmental history. In: Iannone, G. (Ed.), The Great Maya Droughts in Cultural Context: Case Studies in Resilience and Vulnerability, pp. 21–49, 10.5876_9781607322801.C002.

Anselmetti, F.S., Hodell, D.A., Ariztegui, D., Brenner, M., Rosenmeier, M.F., 2007. Quantification of soil erosion rates related to ancient Maya deforestation. Geology 35, 915–918. https://doi.org/10.1130/G23834A.1.

Appleby, P.G., Nolan, P.J., Gifford, D.W., Godfrey, M.J., Oldfield, F., Anderson, N.J., Battarbee, R.W., 1986. 210Pb dating by low background gamma counting. Hydrobiologia 141, 21–27.

Appleby, P.G., 2001. Chronostratigraphic techniques in recent sediments. Basin Analysis, Coring, and Chronological Techniques. In: Last, W.M., Smol, J.P. (Eds.), Tracking Environmental Change Using Lake Sediments, vol. 1. Kluwer Academic Publishers, Dordrecht, pp. 171–203.

Aragon Morreno, A.A., Islebe, G.A., Roy, P.D., Torrescano Valle, N., Mueller, A.D., 2018. Climate forcings on vegetation of the southeastern Yucatán Peninsula (Mexico) during the middle to late Holocene. Palaeogeogr. Palaeoclimatol. Palaeoecol. 495, 214–226. https://doi.org/10.1016/j.palaeo.2018.01.014.

Arnold, T.E., Hillman, A.L., Abbott, M.B., Werne, J.P., McGrath, S.J., Arkish, E.N., 2021.

Drought and the collapse of the tiwanaku civilisation: new evidence from Lake Orurillo, Peru. Quat. Sci. Rev. 251, 106693. https://doi.org/10.1016/j.quascirev.2020.106693.
Bauer-Gottwein, P., Gondwe, B.R.N., Charvet, G., Marín, L.E., Rebolledo Vieyra, M., Merediz Alonso, G., 2011. Review: the yucatan peninsula karst aquifer, Mexico. Hydrogeol. J. 19, 507–524. https://doi.org/10.1007/s10040-010-0699-5.
Beach, T., Dunning, N., Luzzadder-Beach, S., Cook, D.E., Lohse, J., 2006. Impacts of the ancient Maya on soils and soil erosion in the central Maya lowlands. Catena 65, 166–178. https://doi.org/10.1016/j.catena.2005.11.007.
Berger, A., Loutre, M.F., 1991. Insolation values for the climate of the last 10 million years. Quat. Sci. Rev. 10, 297–317. World Data Center for Paleoclimatology, Data contribution series No. 92-007.
Bernal, J.P., Lachniet, M., McCulloch, M., Mortimer, G., Morales, P., Cienfuegos, E., 2011. A speleothem record of Holocene climate variability from southwestern Mexico. Q. Res. 75, 104–113. https://doi.org/10.1016/j.yqres.2010.09.002.
Blaauw, M., Christen, J.A., 2011. Flexible paleoclimate age-depth models using an autoregressive gamma process. Bayesian Anal. 6, 457–474.
Boyle, J.F., 2001. Inorganic geochemical methods in paleolimnology. In: Last, W.M., Smol, J.P. (Eds.), Tracking Environmental Change Using Lake Sediments. Kluwer Academic Publishers, pp. 83–141.
Brenner, M., Rosenmeier, M.F., Hodell, D.A., Curtis, J.H., 2002. Paleolimnology of the Maya lowlands. Anc. Mesoam. 13, 141–157, 10.107.S0956536102131063.
Carillo-Bastos, A., Islebe, G.A., Torrescano Valle, N., González, N.E., 2010. Holocene vegetation and climate history of central quintana roo, yucatán peninsula, Mexico. Rev. Palaeobot. Palynol. 160, 189–196. https://doi.org/10.1016/j.revpalbo.2010.02.013.
Chamberlain, R.S., 1985. Conquista y colonización de Yucatán. In: Castillo Peraza, C. (Ed.), Historia de Yucatán, pp. 105–157 (Dante).
Chase, D.Z., Chase, A.F., 2014. Path dependency in the rise and denouement of a classic Maya city: the case of caracol, Belize. Archaeol. Paper. Am. Anthropol. Assoc. 24, 142–154. https://doi.org/10.1111/apaa.12034.
Chen, N., Bianchi, T.S., McKee, B.A., Bland, J.M., 2001. Historical trends of hypoxia on the Louisiana shelf: applications of pigments as biomarkers. Org. Geochem. 32, 543–561.
Colorado-Ruiz, G., Cavazos, T., Salinas, J.A., De Grau, P., Ayala, R., 2018. Climate change projections from Coupled Model Intercomparison Project phase 5 multi-model weighted ensembles for Mexico, the North American monsoon, and the mid-summer drought region. Int. J. Climatol. 101002/joc.5773.
Conagua, 2014. Informe Final Programa Nacional contra la sequía PRONACOSR. In: Programa de medidas preventivas y de mitigación de la sequía del Consejo de Cuenca Península de Yucatán (PMPMS-CCPY). https://www.gob.mx/cms/uploads/attachment/file/99947/PMPMS_CC_Pennsula_de_Yucat_n_R.pdf.
Conroy, J.L., Overpeck, J.T., Cole, J.E., Shanahan, T.M., Steinitz-Kannan, M., 2008. Holocene changes in eastern tropical Pacific climate inferred from a Galapagos lake sediment record. Quat. Sci. Rev. 27, 1166–1180.
Covich, A., Stuiver, M., 1974. Changes in oxygen 18 as a measure of long-term fluctuations in tropical lake levels and molluscan populations. Limnol. Oceanogr. 19, 682–691.
Cowgill, U.M., Hutchinson, G.E., Racek, A.A., Goulden, C.E., Patrick, R., Tsukada, M., 1966. The history of Laguna Petenxil, a small lake in northern Guatemala. Mem. Conn. Acad. Arts Sci. 17, 1–126.
Curtis, J.H., Hodell, D.A., Brenner, M., 1996. Climate variability on the Yucatan Peninsula (Mexico) during the past 3500 years, and implications for Maya cultural evolution. Q. Res. 46, 37–47.
Curtis, J.H., Brenner, M., Hodell, D.A., Balser, R.A., Islebe, G.A., Hooghmiemstra, H., 1998. A multi-proxy study of Holocene environmental change in the Maya lowlands of Peten, Guatemala. J. Paleolimnol. 19, 139–159.
Dahlin, B.H., 1983. Climate and prehistory on the yucatan peninsula. Climatic Change 5, 245–263.
Davies, S., Lamb, H., Roberts, S., 2015. Micro-XRF core scanning in palaeolimnology: recent developments. In: Croudace, I., Rothwell, R. (Eds.), Micro-XRF Studies of Sediment Cores, Developments in Paleoenvironmental Research, vol. 17. Springer, Dordrecht, pp. 189–221. https://doi.org/10.1007/978-94-017-9849-5_7.
Dean, W.E., 1974. Determination of carbonate and organic matter in calcareous sediments and sedimentary rocks by loss of ignition: comparison with other methods. J. Sediment. Petrol. 44, 242–248.
Deevey, E.S., Rice, D.S., Rice, P.M., Vaughan, H.H., Brenner, M., Flannery, M.S., 1979. Maya urbanism: impact on a tropical karst environment. Science 206, 298–306.
Deevey Jr., E.S., Brenner, M., Binford, M.W., 1983. Paleolimnology of the Peten Lake District, Guatemala III. Late Pleistocene and Gamblian environments of the Maya area. Hydrobiologia 103, 211–216.
Degroot, D., Anchukaitis, K., Bauch, M., Burnham, J., Carnegy, F., Cui, J., de Luna, K., Guzowski, P., Hambrecht, G., Huhtamaa, H., Izdebiski, A., Kleemann, K., Moesswilde, E., Nuepane, N., Newfield, T., Pei, Q., Xoplaki, E., Zappia, N., 2021. Towards a rigorous understanding of societal responses to climate change. Nature 591, 539–550. https://doi.org/10.1038/s41586-021-03190-2.
De la Barreda, B., Metcalfe, S.E., Boyd, D.S., 2020. Precipitation regionalization, anomalies and drought occurrence in the Yucatan Peninsula, Mexico. Int. J. Climatol. 40. https://doi.org/10.1002/joc.6474, 4541-1555.
Douglas, P.M., Pagani, M., Canuto, M.A., Brenner, M., Hodell, D.A., Eglinton, T.I., Curtis, J.H., 2015. Drought, agricultural adaptation, and socio-political collapse in the Maya Lowlands. Proc. Natl. Acad. Sci. Unit. States Am. 112, 5607–5612. https://doi.org/10.1073/pnas.1419133112.
Douglas, P.M.J., Demarest, A.A., Brenner, M., Canuto, M.A., 2016a. Impacts of climate change on the collapse of Lowland Maya civilization. Annu. Rev. Earth Planet Sci. 44, 613–645. https://doi.org/10.1146/annurev-earth-060115-012512.
Douglas, P.M.J., Brenner, M., Curtis, J.H., 2016b. Methods and directions for paleoclimatology in the Maya lowlands. Global Planet. Change 138, 3–24. https://doi.org/10.1016/j.gloplacha.2015.07.008.
Dunning, N.P., Beach, T., 1994. Soil erosion, slope management, and ancient agricultural terracing in the Maya Lowlands. Lat. Am. Antiq. 5, 51–69.
Dunning, N.P., Beach, T., Farrell, P., Luzzadder-Beach, S., 1998. Prehispanic agrosystems and adaptive regions in the Maya Lowlands. Cult. Agric. 20, 87–101.
Dunning, N.P., Beach, T.P., Luzzadder-Beach, S., 2012. Kax and kol: collapse and resilience in lowland Maya civilization. Proc. Natl. Acad. Sci. Unit. States Am. 109, 3652–3657. https://doi.org/10.1073/pnas.1114838109.
Escobar, J., Curtis, J.H., Brenner, M., Hodell, D.A., Holmes, J.A., 2010. Isotope measurement of ostracod and gastropod shells for climate reconstruction: evaluation of within-sample variability and determination of optimum sample size. J. Paleolimnol. 43, 921–938.
Escolero, O., Marín, L.E., Steinich, B., Pacheco, J.A., Molina-Maldonado, A., Anzaldo, J.M., 2005. Geochemistry of the hydrogeological reserve of Merida, Yucatán, Mexico. Geofisc. Int. 44, 301–314.
Evans, N.P., Bauska, T.K., Gazquez-Sanchez, F., Brenner, M., Curtis, J.H., Hodell, D.A., 2018. Quantification of drought during the collapse of the classic Maya civilization. Science 361, 498–501. https://doi.org/10.1126/science.aas9871.
Ford, A., 2008. Dominant plants of the Maya forest and gardens of El Pilar: implications for paleoenvironmental reconstructions. J. Ethnobiol. 28, 179–199.
Fritz, S., 2008. Deciphering climatic history from lake sediments. J. Paleolimnol. 39, 5–16. https://doi.org/10.1007/s10933-007-9134-x.
Fritz, S.C., Bjorck, S., Rigsby, C.A., Baker, P.A., Calder-Church, A., Conley, D.J., 2011. Caribbean hydrological variability during the Holocene as reconstructed from crater lakes on the island of Grenada. J. Quat. Sci. 26, 829–838. https://doi.org/10.1002/jqs.1512.
Gilfedder, B.S., Petri, M., Wesssels, M., Biester, H., 2011. Bromine species fluxes from Lake Constance's catchment, and a preliminary lake mass balance. Geochem. Cosmochim. Acta 74, 3385–3401.
Guttierez-Ayala, L.V., Torrescano-Valle, N., Islebe, G.A., 2012. Reconstrucción paleoambiental del Holoceno tardío de la reserva Los Petenes, Península de Yucatán, Mexico. Rev. Mex. Ciencias Geol. 29, 749–763.
Haug, G.H., Hughen, K.A., Peterson, L.C., Sigman, D.M., Röhl, U., 2001. Southward migration of the intertropical convergence zone through the Holocene. Science 293, 1304–1308.
Hodell, D.A., Curtis, J.H., Brenner, M., 1995. Possible role of climate in the collapse of Classic Maya civilization. Nature 375, 391–394.
Hodell, D.A., Brenner, M., Curtis, J.H., Medina Gonzalez, R., Ildefonso-Chan Can, E., Albornaz Pat, A., Guilderson, T.P., 2005a. Climate change on the Yucatan Peninsula during the Little Ice Age. Q. Res. 63, 109–121. https://doi.org/10.1016/j.yqres.2004.11.004.
Hodell, D.A., Brenner, M., Curtis, J.H., 2005b. Terminal Classic drought in the northern Maya lowlands inferred from multiple sediment cores in Lake Chichancanab. Quat. Sci. Rev. 24, 1413–1427. https://doi.org/10.1016/j.quascirev.2004.10.013.
Hoggarth, J.A., Breitenbach, S.F.M., Culleeton, B.J., Ebert, C.E., Masson, M.A., Kennett, D.J., 2016. The political collapse of Chichén Itzá in climatic and cultural context. Global Planet. Change 138, 25–42, 10.106/j.gloplacha.2015.12.007.
Hoggarth, J.A., Restall, M., Wood, J.W., Kennett, D.J., 2017. Drought and its demographic effects. Curr. Anthropol. 58, 82–113. https://doi.org/10.1086/690046.
Horton, T.W., Defliese, W.F., Tripati, A.K., Oze, C., 2016. Evaporation induced ^{18}O and ^{13}C enrichment in lake systems: a global perspective on hydrologic balance effects. Quat. Sci. Rev. 131, 365–379.
Islebe, G.A., Torrescano Valle, N., Aragón Moreno, A.A., Vela Peláez, A.A., Valdez Hernández, M., 2018. The paleoanthropocene of the Yucatan Peninsula: palynological evidence of Environmental change. Bol. Soc. Geol. Mex. 70, 49–60. https://doi.org/10.18268/BSGM2018v70n1a3.
Ito, E., 2001. Application of stable isotope techniques to inorganic and biogenic carbonates. In: Last, W.M., Smol, J.P. (Eds.), Tracking Environmental Changes Using Lake Sediments.Volume 2: Physical and Geochemical Methods. Kluwer, Dordrecht, pp. 351–371.
Jones, M.D., Imbers, J., 2010. Modelling Mediterranean lake isotope variability. Global Planet. Change 71, 193–200.
Jones, M.D., Abu-Jaber, N., AlShdaifat, A., Baird, D., Cook, B.I., Cuthbert, M.O., Dean, J.R., Djamali, M., Eastwood, W., Fleimann, D., Haywood, A., Kwiecien, O., Larsen, J., Maher, L.A., Metcalfe, S.E., Parker, A., Petrie, C.A., Primmer, N., Richter, T., Roberts, N., Roe, J., Tindall, J.C., Unal-Imer, E., Weeks, L., 2019. 20,000 years of societal vulnerability and adaptation to climate change in southwest Asia. WIREsWater, e1330. https://doi.org/10.1002/wat2.1330.
Juggins, S., 2019. Analysis of Quaternary Science Data Cran (rproject.org/web/packages/rioja/rioja.pdf).
Kennett, D.J., Breitenbach, S.F.M., Aquino, V.V., Asmerom, Y., Awe, J., Baldini, J.U.L., Bartelin, P., Culleton, B.J., Ebert, C., Jazwa, C., Macri, M.J., Marwan, N., Polyak, V., Prufer, K.M., Ridley, H.E., Sodemann, H., Winterhalder, B., Haug, G.H., 2012. Development and disintegration of Maya political systems in response to climate change. Science 338, 788–791. https://doi.org/10.1126/science.1226299.
Kennett, D.J., Hodell, D.A., 2017. In: Weiss, H. (Ed.), AD 750-1100 Climate Change and Critical Transitions in Classic Maya Sociopolitical Networks, Megadrought and Collapse: from Early Agriculture to Angkor. OUP, p. 29. https://doi.org/10.1093/oso/9780199329199.001.0001.
Khan, N.S., Ashe, E., Horton, B.P., Dutton, A., Kopp, R.E., Brocard, G., Engelhart, S.E.,

Hill, D.F., Peltier, W.R., Vane, C.H., Scatena, F.N., 2017. Drivers of Holocene sea-level change in the caribbean. Quat. Sci. Rev. 155, 13–36. https://doi.org/10.1016/j.quascirev.2016.08.032.
Leavitt, P.R., Fritz, S.C., Anderson, N.J., Baker, P.A., Blenckner, T., Bunting, L., Catalan, J., Conley, D.J., Hobbs, W.O., Jeppesen, E., Korkhola, A., McGowan, S., Ruhland, K., Rusak, J.A., Simpson, G.L., Solovieva, N., Werne, J., 2009. Paleolimnological evidence of the effects on lakes of energy and mass transfer from climate and humans. Limnol. Oceanogr. 54, 2330-234.
Leng, M.J., Marshall, J.D., 2004. Palaeoclimate interpretation of stable isotope data from lake sediment archives. Quat. Sci. Rev. 23, 811–831.
Leyden, B.W., 2002. Pollen evidence for climatic variability and cultural disturbance in the Maya Lowlands. Anc. Mesoam. 13, 85–101.
Leyden, B.W., Brenner, M., Whitmore, T., Curtis, J.H., Piperno, D.R., Dahlin, B.H., 1996. A record of long- and short-term climatic variation from northwest yucatán: cenote san josé chulchacá. In: Fedick, S.L. (Ed.), The Managed Mosaic: Ancient Maya Agriculture and Resource Use. University of Utah Press, pp. 30–50.
Leyden, B.W., Brenner, M., Dahlin, B.H., 1998. Cultural and climatic history of Coba, a lowland Maya city in quintana roo, Mexico. Q. Res. 49, 111–122.
Li, H.C., Ku, T.L., 1997. $\delta^{13}C$–$\delta^{18}C$ covariance as a paleohydrological indicator for closed-basin lakes. Palaeogeogr. Palaeoclimatol. Palaeoecol. 133, 69–80.
Marcott, S.A., Shakun, J.D., Clark, P.U., Mix, A.C., 2013. A reconstruction of regional and global temperature for the past 11,300 years. Science 339, 1198–1201.
Medina Elizade, M., Burns, S.J., Lea, D.W., Asmerom, Y., von Gunten, L., Polyak, V., Vuille, M., Karmalkar, A., 2010. High resolution stalagmite climate record from the Yucatan Peninsula spanning the Maya terminal classic period. Earth Planet Sci. Lett. 298, 255–262. https://doi.org/10.1016/j.epsl.2010.08.016.
Medina Elizade, M., Burns, S.J., Polanco-Martinez, Beach, T., Lases Hernandez, F., Shen, C.-C., Wang, H.-C., 2016. High-resolution speleothem record of precipitation from the yucatan peninsula spanning the Maya Preclassic period. Global Planet. Change 138, 93–102. https://doi.org/10.1016/j.globplacha.2015.10.003.
Mendoza, B., Velasco, V., Jauregui, E., 2006. A study of historical droughts in southeastern Mexico. J. Clim. 19, 2916–2934.
Metcalfe, S.E., Barron, J.A., Davies, S.J., 2015. The Holocene history of the North American Monsoon: 'known knowns' and 'known unknowns' in understanding its spatial and temporal complexity. Quat. Sci. Rev. 120, 1–27. https://doi.org/10.1016/j.quascirev.2015.04.004.
Metcalfe, S.E., Schmook, B., Boyd, D.S., De la Barreda-Bautista, B., Endfield, G.E., Mardero, S., Manzon Che, M., Medina Gonzalez, R., Munguia Gil, M.T., Navarro Olmedo, S., Perea, A., 2020. Community perception, adaptation and resilience to extreme weather in the Yucatan Peninsula, Mexico. Reg. Environ. Change 20, 25. https://doi.org/10.1007/s10113-020-01586-w.
Mills, K., Schillereff, D., Saulnier-Talbot, É., Gell, P., Anderson, N.J., Arnaud, F., Dong, X., Jones, M., McGowan, S., Massaferro, J., Moorhouse, H., 2017. Deciphering Long-term Records of Natural Variability and Human Impact as Recorded in Lake Sediments: A Palaeolimnological Puzzle, vol. 4. Wiley Interdisciplinary Reviews: Water, p. e1195.
Mueller, A.D., Islebe, G.A., Hillesheim, M.B., Grzesik, D.A., Anselmetti, F.S., Ariztegui, D., Brenner, M., Curtis, J.H., Hodell, D.A., Venz, K.A., 2009. Climate drying and associated forest decline in the lowlands of northern Guatemala during the late Holocene. Q. Res. 71, 133–141. https://doi.org/10.1016/j.yqres.2008.10.002.
Mueller, A.D., Anselmetti, F.S., Ariztegui, D., Brenner, M., Hodell, D.A., Curtis, J.H., Escobar, J., Gilli, A., Grzesik, D.A., Guilderson, T.P., Kutterolf, S., Plötze, M., 2010. Late Quaternary palaeoenvironment of northern Guatemala: evidence from deep drill cores and seismic stratigraphy of Lake Petén Itzá. Sedimentology 57, 1220–1245. https://doi.org/10.1111/j.1365-3091.2009.01144.x.
Nooren, K., Hoek, W.X., Dermody, B.J., Galop, D., Metcalfe, S., Islebe, G., Middlekoop, H., 2018. Climate impact on the development of Pre-Classic Maya civilisation. Clim. Past 14, 1253–1273. https://doi.org/10.5194/cp-14-1253-2018.
Perez, L., Bugja, R., Lorenschat, J., Brenner, M., Curtis, J., Hoelzmann, P., Islebe, G., Scharf, B., Schwalb, A., 2011. Aquatic ecosystems of the Yucatán Peninsula (Mexico), Belize and Guatemala. Hydrobiologia 661, 407–433. https://doi.org/10.1007/s10750-010-0552-9.
Perry, E., Velazquez Oliman, G., Socki, R.A., 2003. Hydrogeology of the yucatán peninsula. In: Gomez-Pompa, A., Allen, M.F., Fedick, S.L., Jimenez-Osornio, J.J. (Eds.), The Lowland Maya Area. Three Millennia at the Human-Wildland Interface. Food Products Press, pp. 115–138 (Chapter 7).
Pohl, M.D., Pope, K.O., Jones, J.G., Jacob, J.S., Piperno, D.R., deFrance, S.D., Lentz, D.L., Gifford, J.A., Danforth, M.E., Josserand, J.K., 1996. Early agriculture in the Maya lowlands. Lat. Am. Antiq. 7, 355–372.
Pollock, A.L., van Beynen, P.E., DeLong, K.L., Polyak, V., Asmerom, Y., Reeder, P.P., 2016. A mid-Holocene paleoprecipitation record from Belize. Palaeogeogr. Palaeoclimatol. Palaeoecol. 463, 103–111. https://doi.org/10.1016/j.palaeo.2016.09.021.
Poore, R.Z., Dowsett, H.J., Verardo, S., Quinn, T., 2003. Millennial- to century-scale variability in Gulf of Mexico Holocene climate records. Paleoceanography 18, 1048. https://doi.org/10.1019/20002PA000868.
Primmer, N., 2019. Reconstructing High Resolution Environmental Change from Carbonate-Rich Lakes in Turkey and Mexico Using Varve Microfacies Analysis. Unpublished PhD thesis, University of Nottingham.
R Core Team, 2020. R: A Language and Environment for Statistical Computing. R Foundation for Statistical Computing, Vienna, Austria. https://www.r-project.org.
Reimer, P.J., Austin, W.E., Bard, E., Bayliss, A., Blackwell, P.G., Ramsey, C.B., et al., 2020. The IntCal20 Northern Hemisphere radiocarbon age calibration curve (0-55 cal kBP). Radiocarbon 62, 725–757. DOI:10.1017/RDC.2020.41.
Rice, D.S., Rice, P.M., 1984. Lessons from the Maya. Latin Am. Res. 19, 7–34.
Roberts, N., Allcock, S.L., Arnaud, F., Dean, J.R., Eastwood, W.J., Jones, M.D., Leng, M.J., Metcalfe, S.E., Malet, E., Woodbridge, J., Yiğitbaşıoğlu, H., 2016. A tale of two lakes: a multi-proxy comparison of Lateglacial and Holocene environmental change in Cappadocia, Turkey. J. Quat. Sci. 31, 348–362.
Rosenmeier, M.F., Hodell, D.A., Brenner, M., Curtis, J.H., Martin, J.B., Anselmetti, F.S., Ariztegui, D., Guilderson, T.P., 2002. Influence of vegetation change on watershed hydrology: implcations for paleoclimatic interpretation of lacustrine $\delta^{18}O$ records. J. Paleolimnol. 27, 117–131.
Rosenmeier, M.F., Brenner, M., Hodell, D.A., Martin, J.B., Curtis, J.H., Binford, M.W., 2016. A model of the 4000-year paleohydrology ($\delta^{18}O$) record from Lake Salpetén, Guatemala. Global Planet. Change 138, 43–55. https://doi.org/10.1016/j.gloplacha.2015.07.006.
Schmitter-Soto, J.J., Comín, F.A., Escobar Briones, E., Herrera Silveira, J., Alcocer, J., Suárez Morales, E., Elías Gutiérrez, M., Díaz Arce, V., Marín, L.E., Steinich, B., 2002. Hydrogeochemical and biological characteristics of cenotes in the Yucatan Peninsula (S.E. Mexico). Hydrobiologia 467, 215–228.
Sedov, S., Solleiro Rebolledo, E., Fedick, S.L., Gama Castro, J., Palacios Mayorga, S., Vallejo Gomez, E., 2007. Soil genesis in relation to landscape evolution and ancient sustainable land use in the northeastern Yucatan Peninsula, Mexico. Atti della Societa Toscana di Scienze Naturali Serie A 112, 115–126.
Stansell, N.D., Steinman, B.A., Lachniet, M.S., Feller, J., Harvey, W., Fernandez, A., Shea, C.J., Price, B., Coenen, J., Boes, M., Perdiziola, S., 2020. A lake sediment stable isotope record of late-middle to late Holocene hydroclimate variability in the western Guatamala highlands. Earth Planet Sci. Lett. 542, 116327. https://doi.org/10.1016/j.epsl.2020.116327.
Talbot, M.R., 1990. A review of the palaeohydrological interpretation of carbon and oxygen isotope ratios in primary lacustrine carbonates. Chem. Geol. 80, 261–279.
ter Braak, C.J.F., Šmilauer, P., 2012. Canoco Reference Manual and User's Guide: Software for Ordination. Microcomputer Power, version 5.0.
Torrescano-Valle, N., Islebe, G.A., 2015. Holocene paleoecology, climate history and human influence in the southwestern Yucatan Peninsula. Rev. Palaeobot. Palynol. 217, 1–8. https://doi.org/10.1016/j.revpalbo.2015.03.003.
Turner II, B.L., Sabloff, J.A., 2012. Classic period collapse of the Central Maya Lowlands: insights about human-environment relationships for sustainability. Proc. Natl. Acad. Sci. Unit. States Am. 109, 13908–13914. https://doi.org/10.1073/pnas.1210106109.
Turner, R., Roberts, N., Eastwood, W.J., Jenkins, E., Rosen, A., 2010. Climate and the origins of agriculture: micro-charcoal records of biomass burning during the last glacial–interglacial transition in Southwest Asia. J. Quat. Sci. 25, 371–386.
Tylmann, W., Zolitschka, B., Enters, D., Ohlendorf, C., 2013. Laminated lake sediments in northeast Poland: distribution, preconditions for formation and potential for paleoenvironmental investigation. J. Paleolimnol. 50, 487–503. https://doi.org/10.1007/s10933-013-9741-7.
Valero-Garcés, B., Morellon, M., Moreno, A., Corella, J.P., Martín-Puertas, C., Barreiro, F., Pérez, A., Giralt, S., Mata-Campo, M.P., 2014. Lacustrine carbonates of Iberian karst lakes: sources, processes and depositional environments. Sediment. Geol. 299, 1–29. https://doi.org/10.1016/j.sedgeo.2013.10.007.
van Hengstum, P.J., Maale, G., Donnelly, J.P., Albury, N.A., Onac, B.P., Sullivan, R.M., Winkler, T.S., Tamalavage, A.E., MacDonald, D., 2018. Drought in the northern Bahamas from 3300 to 2500 years ago. Quat. Sci. Rev. 186, 169–185. https://doi.org/10.1016/j.quascirev.2018.02.014.
Wahl, D., Byrne, R., Schreiner, T., Hansen, R., 2006. Holocene vegetation change in the northern Peten and its implications for Maya prehistory. Q. Res. 65, 380–389.
Wahl, D., Byrne, R., Anderson, L., 2014. A 8700 year paleoclimate reconstruction from the southern Maya lowlands. Quat. Sci. Rev. 103, 19–25. https://doi.org/10.1016/j.quascirev.2014.08.004.
Walker, M.J.C., Berkelhammer, M., Björck, S., Cwynar, L.C., Fisher, A.J., Lowe, J.J., Newham, R.M., Rasmussen, S.O., Weiss, H., 2012. Formal subdivision of the Holocene series/epoch: a discussion paper by a working group of INTIMATE (integration of ice-core, marine and terrestrial records) and the subcommission on Quaternary Stratigraphy (international commission on stratigraphy). J. Quat. Sci. 27, 649–659. https://doi.org/10.1002/jqs.2565.
Webster, K.E., Soranno, P.A., Baines, S.B., Kratz, T.K., Bowser, C.J., Dillon, P.J., Campbell, P., Fee, E.J., Hecky, R.E., 2000. Structuring features of lake districts: landscape controls on chemical responses to drought. Freshw. Biol. 43, 499–515.
Weldeab, S., Schneider, R.R., Kölling, M., Wefer, G., 2005. Holocene African droughts relate to eastern equatorial Atlantic cooling. Geology 33, 981–984. https://doi.org/10.1130/G21874.1.
Winter, A., Zanchettom, D., Lachniet, M., Vieten, R., Pausata, F.S.R., Charpentier Ljungqvist, F., Cheng, H., Edwards, R.L., Miller, T., Rubinetti, S., Rubino, A., Taricco, C., 2020. Initiation of a stable convective hydroclimatic regime in Central America circa 9000 year BP. Nat. Commun. https://doi.org/10.1038/s41467-020-14490-y.
Witschey, W.R.T., Brown, C.T., 2010. Electronic Atlas of Ancient Maya Sites.
Yan, M., Liu, J., 2019. Physical processes of cooling and mega-drought during the 4.2 ka BP event: results from TraCE-21ka simulations. Clim. Past 15, 265–277. https://doi.org/10.5194/cp-15-265-2019.